The Evolution of the Moon and the Terrestrial Planets

M. Nafi Toksöz and David H. Johnston
Department of Earth and Planetary Sciences
Massachusetts Institute of Technology
Cambridge, Massachusetts

The thermal evolutions of the Moon, Mars, Venus, and Mercury are calculated theoretically starting from cosmochemical condensation models. An assortment of geological, geochemical, and geophysical data are used to constrain both the present-day temperatures and the thermal histories of the planets' interiors. Such data imply that the planets were heated during or shortly after formation and that all the terrestrial planets started their differentiations early in their history.

Initial temperatures and core formation play the most important roles in the early differentiation. The size of the planet is the primary factor in determining its present-day thermal state. The Moon, smallest in size, is characterized as a differentiated body with a crust, a thick solid mantle, and an interior region which may be partially molten. It is presently cooling rapidly and is relatively inactive tectonically.

Mercury, which probably has a large core, may have a 500-km-thick solid lithosphere and a partially molten core, if it is assumed that some heat sources exist in the core. If this is not the case, the planet's interior temperatures are everywhere below the melting curve for iron. The thermal evolution is dominated by the core separation and the high conductivity of iron that makes up the bulk of Mercury.

Mars, intermediate in size, is assumed to have differentiated an Fe-FeS core. While the formation of an early crust is evident, large-scale melting and differentiation of the mantle silicates has occurred at least up until 1 b.y. ago. Present-day temperature profiles indicate moderate tectonic activity at the present time.

Venus is characterized as a planet not unlike the Earth in many respects. Core formation has occurred probably during the first billion years after the formation. The present-day temperatures indicate a partially molten upper mantle overlain by a 100-km-thick lithosphere and a molten Fe-Ni core. We can expect that today Venus may have tectonic processes similar to the Earth's.

The evolution of a planetary body is very strongly controlled by its thermal regime. Differentiation, volcanism, tectonic activity, and even magnetic field are all processes controlled by the internal temperatures and the thermal history. The calculation of the thermal evolution, however, requires strong constraints if it is to be realistic. In recent years significant new data from lunar and planetary missions have become available. For the Moon these have provided constraints both on the present-day temperatures and the past history of the thermal state of the lunar interior. For Mars, Venus, and Mercury, the thermal constraints are primarily qualitative. The purpose of this paper is to review these data and the thermal evolution models of the Moon and the terrestrial planets.

An extensive number of studies on thermal history of the Moon and planets have been carried out (refs. 1 through 34).

In the early studies, the Moon and the planets were generally modeled with chondritic compositions and radioactivity. With the successful lunar missions and new geo-

chemical data, it became necessary to revise the constraints used in lunar thermal calculations. The models generated since 1971 have incorporated these new data and in general give similar results. Generally, calculations for the other planets reflect this new knowledge about the chemistry of the solar system.

In this paper, then, we present thermal evolution models for the Moon, Mars, Venus, and Mercury for a comparative study. We use similar computational techniques and thermal factors associated with melting, differentiation, and core formation. These are discussed first. The thermal evolution of the Moon, with appropriate constraints, is then presented, followed by a discussion of the thermal evolution of the planets.

Computational Procedure and Model Parameters

For the theoretical calculations of thermal evolution in a planetary body, it is necessary to specify the initial conditions, heat sources, heat transport mechanisms, and a number of other parameters such as specific heat, density, and melting temperatures, as well as variations of these with temperature and pressure inside the planet. Generally, not all of these parameters can be determined and theoretical calculations cannot define thermal models uniquely.

The first input in theoretical calculations is the initial conditions assumed. Included in this is the heating due to accretion, tidal forces, induced electric currents, and short-lived radioactivity, although the relative importance of each may vary. Next is the definition of the long term heat sources that are important throughout the age of the planet. These include heating due to the decay of radioactive isotopes and the possibility of long term heating due to tidal dissipation and electrical currents. Finally, using the above inputs combined with other physical parameters, the conservation of energy equation must be solved numerically with the addition of certain perturbations designed to simulate melting, differentiation, and convection.

In this section we first describe the input parameters and then discuss the computational procedures involved in solving the thermal evolution problem.

MODEL PARAMETERS

Initial Temperature

The initial temperature of a planet is a function of both its mode of formation and its immediate environment during and shortly after its origin. As will be discussed in the following sections, constraints on lunar and planetary thermal evolution favor initially hot and possibly molten models. This is especially true for the Moon. Energy sources which might have provided the heat to raise the temperature of the planets to solidus or near-solidus levels include gravitational energy due to accretion, tidal dissipation, solar wind flux, short-lived radioactivity, and heating due to adiabatic compression. The temperature rise due to adiabatic compression amounts to only a few tens of degrees in the Moon, but increases with the increasing size of the planet. The effect of short-lived radioactivity depends on the time between nucleogenesis and lunar formation. Also, Schramm et al. (ref. 35) have shown that Al^{26}, the most likely heat source in the early history of the solar system (ref. 36), had little effect on the initial heating of the Moon and meteorites.

Tidal dissipation and solar wind flux could have been effective under special circumstances. The amount and the distribution of heat is difficult to quantify in both cases. For the Moon, as an example, the effects of tidal dissipation would be small (ref. 37), unless the Moon's orbit was originally much closer to the Earth. This might have occurred shortly after a capture event or after the Moon formed in close proximity to the Earth (ref. 38). Hallam (ref. 39) has calculated that tidal dissipation, even with $Q = 10$, raises the internal temperature by only 50–

100K in 1.5 b.y. Even if the Moon was once close to the Roche limit, it would recede so rapidly that the effect of tidal heating would be negligible.

Heating by electric currents produced by a unipolar generator driven by the solar wind might have been significant if the Sun had passed through a T-Tauri stage (ref. 40). This effect is difficult to calculate and include explicitly in any thermal model. However, combinations of all the above effects may contribute to the initial temperatures. We considered these effects by means of a "base" temperature added to accretional thermal profiles discussed below.

The most promising initial heat source for the terrestrial planets is the gravitational energy of accretion. Classically this effect is described by the equilibrium of added gravitational potential energy with black body radiation and internal heat:

$$\rho\frac{GM(r)}{r}dr = \varepsilon\sigma(T(r)^4 - T_b^4)\,dt + \rho C_p(T(r) - T_b)\,dr \qquad (1)$$

where t is time, ρ is the density of the accreting particles, G is the gravitational constant, $M(r)$ is the mass within radius r, σ is the Stefan-Boltzmann constant, C_P is the specific heat, and ε is the emissivity (taken to equal 1). $T(r)$ is the temperature at radius r, and T_b is the base temperature or the temperature of the accreting particles, including any effects of short-lived radioactivity. By specifying the accretion rate dr/dt and the physical parameters ρ, C_p, and T_b, temperature versus depth for an accreted body can be calculated from equation (1). An accretion rate suggested by Hanks and Anderson (ref. 15) and Mizutani et al. (ref. 41) is used in this paper and is given by:

$$\frac{dr}{dt} = ct^2 \sin \gamma t \qquad (2)$$

The constants c and γ are determined from the planet's final radius and the duration of accretion. Although the accretion rate is difficult to establish, it is a fair statement of the presumption that the rate grows as the accreted body grows, and that the rate then tapers off as primary material is depleted.

The accretion time is considered arbitrary, except that it is assumed to be longer for larger planets. Generally the accretion time and T_b are adjusted to provide an initial temperature profile consistent with the constraints that require initial differentiation. For the Moon, it can be shown from equations (1) and (2) that the temperature will never reach the basalt solidus for accretion times greater than 1000 years, unless the emissivity of the lunar surface is decreased. This conclusion was reached independently by Mizutani et al. (ref. 41) from a more detailed study of the accretion process.

Heat Sources

The most important long term heat source in thermal history calculations is the heat generated from the decay of the long half-life radioactive isotopes U^{238}, U^{235}, Th^{232}, and K^{40}. Abundances of these isotopes have been measured in many Earth rocks and returned lunar samples (refs. 42 through 48, and others), and indirectly by lunar orbital γ-ray spectrometers (ref. 49). While surface concentrations vary greatly, we may conclude that these values must be much higher than those in the interior of the Earth or the Moon (ref. 50, and others). The distribution of the isotopes in space and time are difficult to constrain, however, due to complex melting and crystal-liquid fractionation processes.

Figure 1 shows total K and U abundances measured for Apollo samples (including crystalline rocks, soils, and breccias), some meteorites, and terrestrial rocks. Figure 2 shows Th/U versus U for the same suite of measurements. Although there are small and systematic deviations, the K/U ratio for lunar material averages around 2000, compared with 10 000 for terrestrial rocks and 80 000 for chondrites. The low lunar K/U ratio is consistent with general depletion of volatile elements (refs. 42 and 52). From this, it is clear that neither terrestrial nor chondritic abundances can be used as the bulk radioactivity for the Moon. Furthermore, using

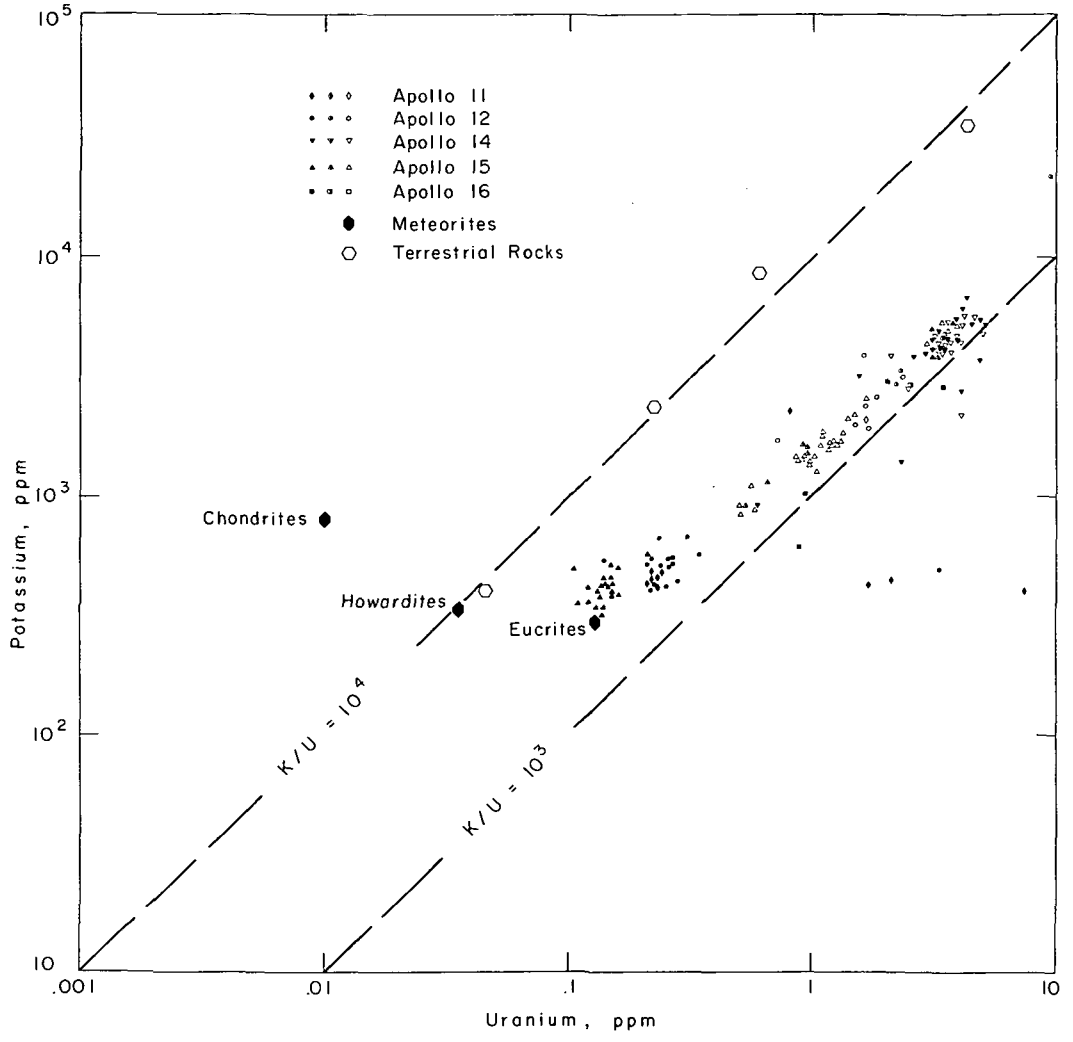

Figure 1.—*Potassium and uranium concentrations in selected meteorites, lunar samples, and terrestrial rocks. Lunar rocks are separated into three categories: crystalline rocks represented by filled symbols, breccias shown by half-filled symbols, and fines shown by empty symbols. Points for average chondrites, howardites, and eucrites are from Mason (ref. 51). Sources for lunar values are given in the text.*

Rb abundances for a model of the primitive lunar material (ref. 18), we can also reject chondrites. The Th/U ratio is consistently between 3.0 and 4.0 for terrestrial, lunar, and meteoritic material.

It is essential, then, to determine or estimate the bulk radioactive concentrations for each of the planets. In the case of the Moon, given that chondrites and terrestrial rocks are not good approximations of the bulk radioactivity, we turn to achondrites—specifically howardites and eucrites. A genetic relationship between achondrites and the Moon has been suggested by several investigators (refs. 53, 54, and 55). Howardites have, on the average, a uranium concentration of 35 ppb, with K/U = 9800, while brecciated eucrites, enriched in refractory elements, have U = 130 ppb, with K/U = 2300 (ref. 51). It is interesting to note that the K/U ratio for eucrites is close to that of the lunar material, while the ratio for howardites is somewhat higher.

If we take K/U for the bulk radioactive

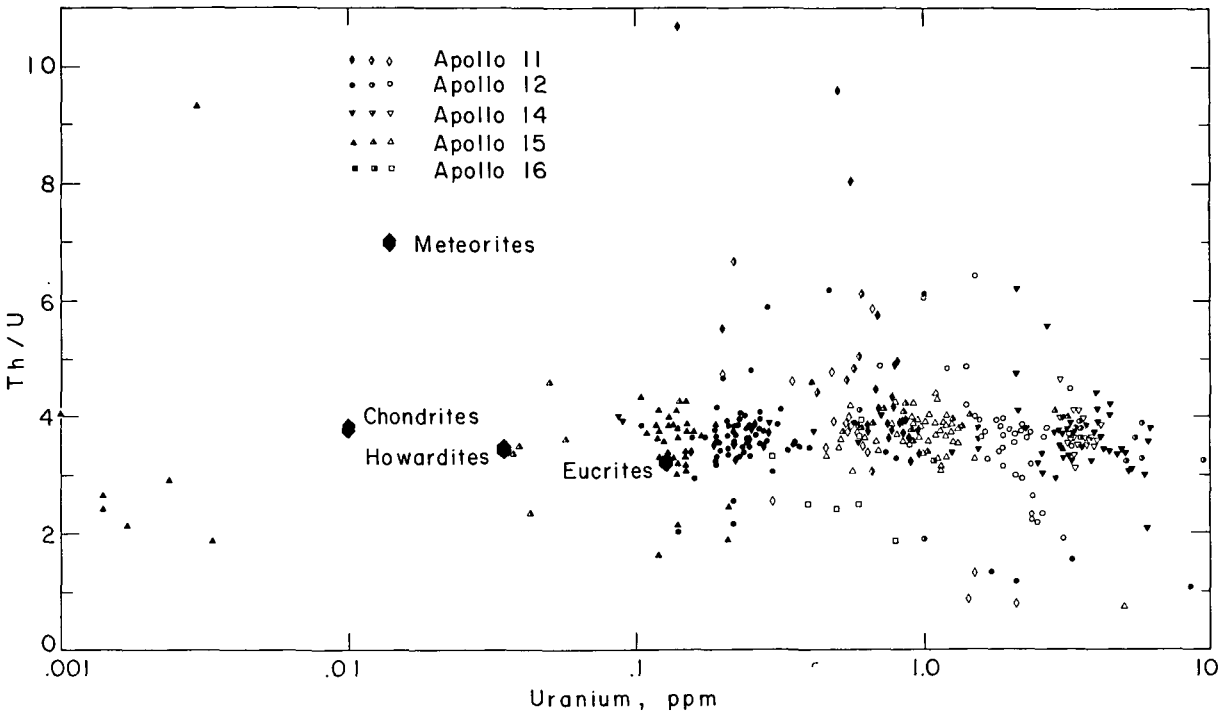

Figure 2.—*Th/U ratio versus uranium concentration for selected lunar rocks and meteorites. Lunar rocks are divided into crystalline rocks, breccias, and fines, with the same notation as in figure 5. Points for average chondrites, howardites, and eucrites are from Mason (ref. 51). Sources for lunar values are given in the text.*

concentration of the Moon to be 2000 and Th/U to be 3.5, then the average radioactivity of the Moon is a function of the bulk uranium content. Given the measured Apollo 15 and 17 heat flows of about 30 ergs/cm^2-s (refs. 56 and 57), Toksöz and Solomon (ref. 30) have shown that the bulk uranium concentration must be 60 $\pm$ 15 ppb to match the heat flow value. In this paper, then, we let U = 60 ppb, with K/U = 2000 and Th/U = 3.5 for the Moon.

For Mars, Venus, and Mercury, we will utilize values based on condensation models of the solar nebula (refs. 54, 58, and 59). These are shown in table 1. In the calculations we consider variations for individual cases as discussed in later sections. However, we expect that for Venus terrestrial abundances are a good approximation. For Mars we use values between terrestrial and chondrite abundances (ref. 32). For Mercury the uranium values are close to those of the Moon, but the planet is most likely lacking in K^{40} (ref. 33). The relevant decay constants, decay energies, and isotopic abundances are taken from Clark (ref. 60).

Distribution of Heat Sources

In most cases, the thermal models presented in this paper assume an initially homogeneous distribution of heat sources. However, the constraints on the internal temperatures rule out, at least for the Moon, a present-day uniform distribution of heat sources. When melting occurs, one would expect the magma to be enriched in U, Th, and K and to subsequently transfer these heat sources to the surface. To account for this, at discrete time steps the heat sources from the molten zones are differentiated upwards, leaving primordial radioactive abundances in any solid region below the zone. Heat

Table 1.—*Parameters Used in Thermal History Calculations*

	Mercury	Venus	Moon	Mars
Radius (km)	2439	6050	1738	3389
Mean Density (g/cm^3)	5.43	5.25	3.34	3.96
C/Ma^2	—	—	0.394	0.377
Surface Temperature (°C)	77	327	−20	−40
Uranium, ppb	44	31	60	31 [a]
K/U ratio	[a]	10,000	2000	10,000 [a]
Th/U ratio	4	4	3.6	4
Specific Heat (silicates) (J/g°C)	1.2	1.2	1.2	1.2
Heat of Fusion (silicates) (J/g)	400	400	400	400

NOTE: (1) See text.

sources differentiated toward the surface are allowed to decrease exponentially with depth so that

$$H(r) = A_0 \exp\left[-\frac{(R-r)}{h}\right] \quad (3)$$

where A_0 is the surface abundance, R is the radius, and $H(r)$ is the radioactive abundance at radius r. Such a distribution has been formulated for the Earth (ref. 61). The skin depth h decreases with time and is adjusted so that the present-day surface radioactivity, if known, is approximated.

Thermal Conductivity and Other Parameters

In a differentiating planet, heat is transported by conduction and by convection. At temperatures far below solidus, the role of convective flow is small and heat transport is governed by thermal conductivity. This quantity is temperature-dependent and is taken to be the sum of two terms, lattice (or phonon) conductivity and radiative conductivity. The relative dominance of each term is of crucial importance in solving the conduction problem of the planets. Although effective thermal conductivities have been measured for terrestrial and lunar materials (fig. 3), these do not always represent the bulk properties of the Moon or planetarv interiors. MacDonald's (ref. 8) theoretical formulation of conductivity as a function of temperature assumed the opacity to be constant, resulting in a cubic temperature dependence of the radiative term and, thus, its dominance over all temperatures. However, Schatz and Simmons (ref. 64) proposed that for a hypothetical dunite, radiative transfer is suppressed by grain-boundary extinction, resulting in an increase in the opacity with temperature. At low temperatures, then, the effective conductivity is dominated by the lattice term that decreases with increasing temperature. At higher temperatures, the radiative term, increasing roughly linearly with temperature, becomes dominant. This model has been used in previous thermal history calculations at MIT (refs. 23 and 30). For the Moon, however, upon examination of figure 3 and values of conductivity in many previous lunar models, one could just as well take the effective conductivity to be a constant. In some of the lunar models and for Mercury's mantle we shall treat it thus, with $K = 0.45 \times 10^6$ ergs/cm-s °C, while other calculations assume the model of Schatz and Simmons (ref. 64). The total conductivity, K, is given by

$$K = K_L + K_R$$

where K_L = lattice conductivity and K_R = radiative conductivity. As functions of temperature, T, these are given by

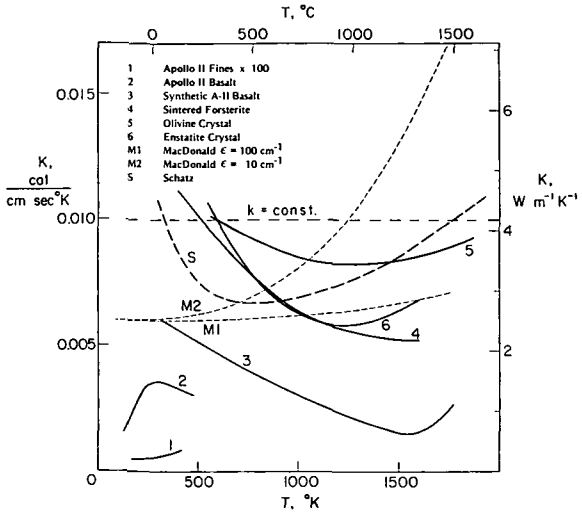

Figure 3.—*Thermal conductivity of selected materials. Sources of measured data (solid lines) are Cremers (ref. 62) for Apollo 11 fines, sample density 1.64 g/cm³; Horai et al. (ref. 63) for Apollo 11 basalt; Murase and McBirney (1970) for synthetic Apollo 11 basalt; Schatz and Simmons (ref. 64) for sintered, polycrystalline forsterite and for single crystal olivine (Fo_{86} Fa_{14}) and enstatite. Theoretical (dashed) curves include those of MacDonald (ref. 8) for two different values of the opacity ϵ, and one proposed by Schatz and Simmons (ref. 62) for polycrystalline olivine of approximate composition $Fo_{90}Fa_{10}$. The Schatz and Simmons curve, labeled S above and K = constant, was employed in this paper.*

$$K_L = \frac{4.184 \times 10^7}{30.6 + 0.21T}$$

and

$$K_R = \begin{cases} 0 \text{ for } T \leq 500°\text{K} \\ 230(T\text{-}500) \text{ for } T > 500°\text{K} \end{cases}$$

Other physical parameters required for the calculations are the melting curve, surface temperature, specific heat, heat of fusion, and density. A summary of the parameters common to all models is given in table 1. Appropriate melting curves are used for each planet, taking into account the composition and pressure.

COMPUTATIONAL TECHNIQUES

In this section we describe the thermal calculations for a spherically symmetric planet, taking into account conduction, melting, simulated convection of molten material, and differentiation.

Conductive Models

Assuming that conduction is the only mode of heat transfer in solid material (an approximation to convection will be discussed later), thermal evolution models are calculated using the finite difference solution of the heat conduction equation:

$$\rho C_p \frac{\partial T}{\partial t} = \frac{1}{2}\frac{\partial}{\partial r}\left(r^2 K \frac{\partial T}{\partial r}\right) + H(r,t) \quad (4)$$

where C_p is the specific heat, T is the temperature, r is the radius, K is the thermal conductivity, and $H(r,t)$ is the heat source term. The latter two quantities were discussed above.

The details of the calculations are described fully in the appendix of Toksöz et al. (ref. 23) and are stated here briefly. The finite difference analog of equation (4) which conserves heat flux is

$$T_n^{m+1} = T_n^m + \frac{\alpha}{n^2 p^2}\left[\left(n+\frac{1}{2}\right)^2 \frac{(K_{n+1}^m + K_n^m)}{2}(T_{n+1}^m - T_n^m) - \left(n-\frac{1}{2}\right)^2 \frac{(K_n^m + K_{n-1}^m)}{2}(T_n^m - T_{n-1}^m)\right] + \alpha H_n^m \quad (5)$$

where $\rho = \Delta r$, $r = np$, $t = m\Delta t$, $\alpha = \Delta t/\rho C_p$, and $T_n^m = T(np, m\Delta t)$. The stability condition relating the time increment and the grid spacing is

$$\Delta t < \frac{C_p \rho \Delta r^2}{2 K_{\max}} \frac{n^2}{\left(n+\frac{1}{2}\right)^2} \quad (6)$$

where $K_{\max}$ is the maximum value of the conductivity at a given time step. Δt is computed at each iteration using equation (6), with a factor of 4 instead of 2 in the denominator. A grid spacing, Δr, of 20 km is used.

Boundary conditions for the problem require the surface temperature of the planet to be constant, and $T_1^m = T_2^m$, where T_1^m is the

temperature at $r_1 = \Delta r$ and T_2^m is the temperature at $r_2 = r_1 + \Delta r$. The solution starts at $r = \Delta r$ to avoid a singularity at $r = 0$. Surface heat flux is calculated by adding the heat flow at the boundary between the upper two finite difference cells to the steady-state heat flow due to heat production in the uppermost half cell.

Simulation of Melting and Convection

The effects of melting and convection of molten material on temperature within the body can be modeled following the technique described by Reynolds et al. (ref. 65). In this method the temperature at each grid point at each time step is compared to the melting temperature at the respective grid point. If the temperature is greater than the melting point, the difference divided by the density and specific heat gives the heat equivalent, ΔH. If ΔH is less than or equal to the heat of fusion, ΔH_f, the material at that grid point is considered partially molten, and the temperature is set equal to the melting point. This process is continued at each iteration until the accumulated ΔH is greater than ΔH_f. At this point in time, the material is considered to be completely molten and the temperature is allowed to rise above the solidus. The same process allows completely molten material to solidify, releasing heat equal to ΔH_f.

In simulating convection of molten material, the same technique as outlined above is followed, with the exception that the temperature of the completely molten material is constrained to the melting curve. Any increase in temperature that would raise the temperature above the melting point is converted to its heat equivalent, transferred upward to the next grid point, and considered to be a temperature rise due to convection. The conversion to heat equivalents is necessary due to the increase in the volume element with increasing radius. The advantage of this approximation to convection is that it does not require the inclusion of mass transfer terms in the heat conduction equation. This scheme is not limited to convection of completely molten material. Convection of partially molten material is easily approximated by reducing the heat of fusion. Convection by solid-state creep requires techniques different from those described above. Various attempts at approximating solid-state convection and determining its relative effect on the thermal evolution of the Moon and planets are discussed in the following section.

SOLID STATE CONVECTION

The question of whether or not thermal models calculated assuming conduction mechanisms are unstable to solid-state convection motions has been discussed in many papers, most recently by Tozer (refs. 24 and 25), Turcotte et al. (ref. 66), Cassen and Reynolds (refs. 29 and 67), and Schubert et al. (ref. 34). Much of this work has been motivated by Schubert et al. (ref. 68). Using a number of conduction temperature profiles for the planets, these investigators applied a linear stability analysis and concluded that thermal convection would occur in each case. Earlier, Runcorn (refs. 69 and 70) attempted to explain departures of the lunar surface from hydrostatic equilibrium by employing convection. Whether or not convection has played a dominant role in the evolution of the planets, however, is still debatable. The question is not easily answered, since the presence (or absence) of convection is a complex function of the temperature and the rheology of the planetary material. Futhermore, in the case of the Moon, the characteristics of the mare basins and their possible filling with basalts by gravitational upwelling of magma implies the presence of more complicated geometries than the simple cellular convection pattern postulated by some investigators. Such upwelling type heat transport is well approximated in our calculations described earlier. Also, the attenuation of shear waves and the presence of deep moonquakes in the lunar interior, as discussed in the following section, present

difficulties for those who hypothesize that solid-state convection occurs in the Moon.

The strongest advocate for the dominance of solid-state creep in the Moon and planets has been Tozer (refs. 24, 25, and 26). In all his papers, Tozer has postulated that convection is at least as important as conduction for any planetary body of radius greater than a few hundred kilometers. This theory, based on the assumption that at any finite temperature an arbitrarily small nonhydrostatic stress produces some permanent deformation of the material, suggests that at some viscosity, or range of viscosities, this motion, or rate of creep, becomes "fast" enough to provide a very efficient method of heat transfer.

In this paper we do not go into detailed convection calculations. In some cases, however, we include models that approximate solid-state creep by arbitrarily raising the thermal conductivity of material with temperatures above a certain threshold value.

Thermal Evolution of the Moon

CONSTRAINTS ON THERMAL EVOLUTION

Thermal evolution calculations generally require boundary conditions that would indicate directly or indirectly the temperatures at certain times inside the planetary body. In addition to these, data are needed to specify material behavior, heat transport mechanisms, and heat sources. Normally, insufficient data and constraints are available. Thus, calculations generally are carried out with a set of initial conditions and assumptions, and the conditions are modified if the temperature models fail to satisfy available constraints.

Data and samples from Apollo missions imposed some strong constraints on the thermal evolution of the Moon. Some of these, such as heat flow, electrical conductivity, seismic velocities, attenuation, and tectonism, pertain to present-day temperatures. Some others, such as the presence of a differentiated lunar crust and chronology of lunar igneous and magmatic activity, indicate the thermal state early in the lunar history.

Lunar Heat Flow

Two heat flow measurements have been made on the Moon, one each at the Apollo 15 (Hadley Rille) and Apollo 17 (Taurus-Littrow) sites. The experiments and their results are described by Langseth et al. (ref. 57). The heat fluxes have been determined by measuring temperature gradients and thermal conductivities in bore holes to a maximum depth of 234 cm. In that depth range, temperature gradients in the lunar regolith are between 1.3 and 1.7 °K/m, and the thermal conductivity is in the range 1.7×10^{-4} and 2.0×10^{-4} W/cm-°K. The heat flow through the surface based on the measured temperature gradients and conductivity is 31 ergs/cm^2-s at the Apollo 15 site and 28 ergs/cm^2-s at the Apollo 17 site (ref. 57). In each case the estimated uncertainty is about $\pm$ 20 percent.

The Taurus-Littrow and Hadley Rille sites are located in the basalt-flooded valleys at the rims of the Serenitatis and Imbrium basins, respectively. There are no direct data to suggest that the thermal characteristics of these sites are any different from other parts of the Moon. Thus, an average heat flow value of about 30 ergs/cm^2-s will be adopted for the Moon in these calculations. This value is about one-half the average heat flow of the Earth (63 ergs/cm^2-s). If we assume steady-state conditions for both bodies and take into account the differences in the radii (average radii: $R_{Moon} = 1738$ km, $R_{Earth} = 6371$ km), surface area ($S_{Moon}/S_{Earth} = 0.074$), and volume ($V_{Moon}/V_{Earth} = 0.02$), we find that the lunar heat flow is higher by about a factor of 2 compared to the Earth. As was discussed earlier in this paper, this implies higher heat generation and radioactive sources inside the Moon than inside the Earth.

Another important measurement arising from the heat flow experiments is the value

of the near-surface temperature. At a depth of about 70 cm, the measured average ambient lunar temperature is 253 K. This will be used as the surface temperature in our calculations.

Electrical Conductivity and Inferred Temperatures

Three magnetometers deployed on the lunar surface, one each at the Apollo 12, 15, and 16 sites, have recorded the magnetic fields induced in the Moon by large-scale transient events. In addition to these, the ambient and time-dependent magnetic fields in the lunar environment are measured by the Explorer 35 satellite magnetometer which is orbiting the Moon.

The analysis of the transient fields recorded simultaneously by the Explorer 35 magnetometer and the surface magnetometer has made it possible to calculate the electrical conductivity inside the Moon (refs. 71 through 74). The Moon responds to transient magnetic events which induce eddy currents in the lunar interior. The response or transfer function is computed from the induced field at the Moon's surface and the forcing (source) function recorded by the Explorer 35 magnetometer.

These results are interpreted by calculating the theoretical response of the Moon with radially varying conductivity. Although there are some limitations of the theoretical calculations and some difficulty in matching all the available data, the results definitely show an increase of electrical conductivity with depth into the Moon. To a depth of about 1000 km the conductivity profile can be characterized by three layers (ref. 72) or by a greater variety of models including current layers (ref. 74). The resolving power of the data is not sufficient to detail the conductivity below this depth.

Conductivity depth profiles given by Dyal et al. (ref. 72) and the three-layer model (a good representation for the average models) of Sonett et al. (ref. 74) are shown in figure 4. Basically, the models require very low conductivity ($\sigma_1 \leq 10^{-9}$ mho/m) for the outer 50 km of the Moon. For the intermediate layer ($1100 < R \leq 1700$ km; R is radius), the conductivity is in the range of $\sigma_2 = 1$ to 7×10^{-4} mho/m. For the deeper interior there is a greater discrepancy. While Sonett et al. (ref. 74) give a value of about $\sigma_3 \simeq 10^{-3}$ mho/m for $R < 1200$ km from the sunlit side data, Dyal et al. (ref. 72) give $\sigma_3 \cong 10^{-2}$ for $R \leq 1000$ km.

From the conductivity profiles, the temperatures inside the Moon can be estimated if the composition and temperature depen-

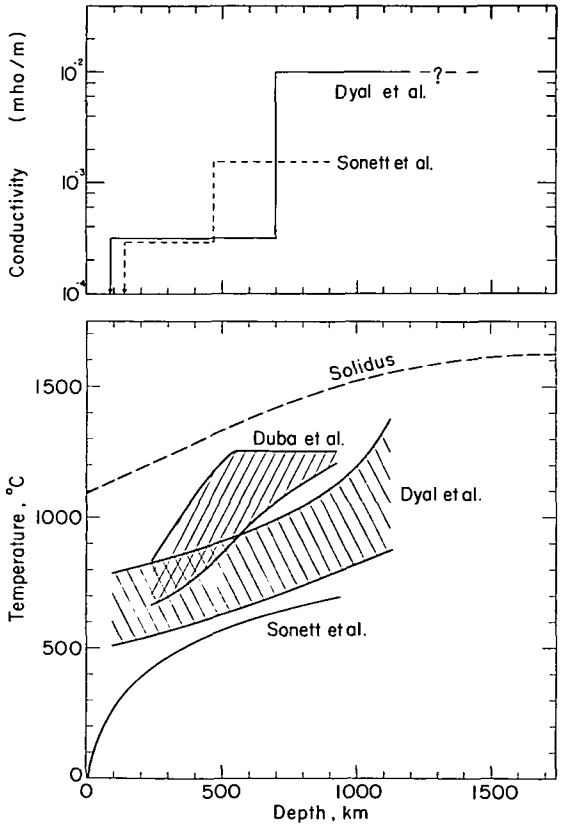

Figure 4.—*Lunar electrical conductivity profiles of Sonett et al (ref. 74) and Dyal et al. (ref. 72) and some estimates of present-day temperatures in the Moon inferred from these measurements. Included are the temperature curve of Sonett et al. (ref. 73), an interpretation of the Sonett et al. (ref. 73) conductivity distribution using the temperature-conductivity relation of an olivine with little or no Fe^{3+} (ref. 28), and the estimates by Dyal et al. (ref. 71) based on their conductivity models.*

dence of conductivity are known. For a given composition, conductivity, σ_T, increases with temperature: $\sigma_T = \sigma_0 \exp\left(-\frac{A}{kT}\right)$, where A = activation energy, k = Boltzmann constant, T = absolute temperature, and σ_0 is a constant dependent on the material. If olivine were assumed for a composition and a lower bound on the conductivity of olivine is used, a temperature of about 1000°C is estimated for the Moon at about 700 km depth (refs. 72 and 74). If newer laboratory data on pyroxenes and olivines—the most likely candidates for mantle composition (refs. 28, 75, and 76)—are used, higher temperatures (i.e., 1000°C at 400 km and 1400° at 800 km depth) are estimated (refs. 28 and 77). Some bounds on temperature models are shown in figure 4; in all cases temperatures are below the solidus to a depth of about 600 to 700 km. At greater depths, temperatures either approach or exceed the solidus, or some changes in the composition increase the conductivity. Another feature of this deep region is that both conductivity and temperature profiles flatten.

Structure of the Lunar Interior and Seismic Wave Attenuation

Seismic studies of the Moon have revealed much valuable information on the structure and the rheological properties of the lunar interior. The presence of a layered structure indicates differentiation and melting in the past. The attenuation characteristics of seismic waves may be explained in terms of increased temperatures or partial melting at the present.

The seismic velocity structure for the outer 150 km of the Moon has been determined from the analysis of manmade impact seismograms recorded by the Lunar Seismic Network (refs. 78, 79, and 80). This structure shows the presence of a lunar crust overlying a mantle. Over the mare the crust may be two layered (the upper layer being mare basalt), with a total thickness of about 60 km. In the highlands and on the backside, the crust may be somewhat thicker. The compositional inferences that can be made from the velocities and other data suggest that the crust is chemically different from the mantle and that it may have formed by the upward differentiation of the lighter minerals.

Below the crust the lunar mantle may extend to a depth of about 1000 km, probably with nearly constant compressional velocities (refs. 81 and 82). Data from moonquakes and meteorite impacts specify the properties of the mantle. The recording of well-defined shear waves from the deep moonquakes implies that the mantle must be sufficiently rigid to 700 or 1000 km depth to prevent appreciable shear-wave attenuation.

Seismic shear waves from farside impacts and farside moonquakes that have penetrated deeper into the Moon than about 700 km are attenuated (refs. 82, 83, and 84). This indicates a possible "softening" of the material in the central region of the Moon below about 700 or 1000 km. Any softening that would reduce Q to less than about 500 would explain the observations. This could be achieved by temperatures approaching the solidus, by a very small amount of partial melt, or by other mechanisms (such as perhaps an increase in the amount of volatiles in the deep lunar interior or a different bulk composition).

If we assume that the attenuation is due to temperature effects, this would place some limits, within the compositional constraints, on the temperatures below 700 km in the Moon. For a pyroxene-olivine-rich composition this is 1600°C. If the Moon has an Fe-FeS-rich core (see ref. 85 for a discussion), the minimum temperature for it would be about 1000°C, given by the Fe-FeS eutectic. Thus, the present-day lunar "core" temperatures range from about 1000 to 1600°C.

Constraints Implied by Lunar Viscosity, Seismicity, and Mascons

The lunar interior described in the previous section and shown in figure 5 can be divided into three units: a crust, a relatively rigid 1000-km-thick "lithosphere," and a

relatively soft deep interior "asthenosphere."

The crust and the lithosphere have supported lunar mass anomalies ("mascons") for over 3 b.y. This requires that (1) at the time of the mascon formation and mare flooding the lunar lithosphere was thick enough to support the loads (ref. 86) and (2) the viscosity of the lithosphere must be greater than about 10^{26} poise (refs. 87 and 88). This high viscosity requires temperatures significantly lower than the melting curve in the outer few hundred kilometers of the Moon.

Another important constraint on the present-day thermal state is that the lunar interior is the very low level of seismic activity in the Moon. Total seismic energy release in the Moon is about 10^{11} ergs/yr, 13 orders of magnitude lower than that of the Earth (refs. 83, 89, and 90). All moonquakes are very small, and those whose focal depths can be determined have hypocenters between 700 and 1200 km depth. These indicate that if there is any convection or tectonic motion taking place in the Moon today, it must be below about 700 to 1000 km.

Chronology of Lunar Igneous Activity

The time history of differentiation and igneous activity imposes the strongest constraints on the early thermal state of the Moon. The chronology of the lunar igneous activity starts from the formation of the original crust about 4.6 b.y. ago as deduced from model ages of lunar rocks and soils (refs. 91 through 94). More recently a Rb-Sr age of 4.6 b.y. has been obtained for an Apollo 17 dunite fragment (72415) by Albee et al. (ref. 95). To create a 60-km-thick feldspathic crust described in the previous section requires the total or partial melting and differentiation of at least one-half of the total volume of the Moon (ref. 96). This requirement strongly constrains the initial temperature of the lunar interior.

Following the formation of the initial crust, the chronology of lunar rocks (an excellent summary has been compiled by Doe (ref. 97)) is defined by three episodes in the lunar evolution:

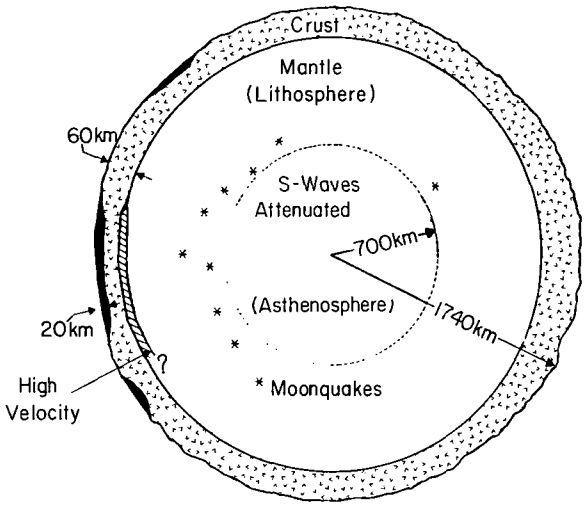

Figure 5.—*Schematic diagram of the structure of the Moon as inferred from lunar seismic data (ref. 80).*

1. The period 4.4 to 4.0 b.y. ago was characterized by continuing igneous activity, brecciation by meteoritic bombardments, and metamorphism of the older rocks. Because of the subsequent events, the detailed record of this episode has been largely obscured. Available data include ages of anorthosites (4.1 b.y. for lunar rock 15415) (ref. 98), the formation ages of KREEP basalts (refs. 50 and 99), and a number of the "recrystallization" ages of the metamorphosed breccias from the Apollo 12, 14, 16, and 17 and Luna 20 sites (see ref. 97 for a compilation). These are shown in figure 6.
2. Episode of basin excavation (4.0 to 3.9 b.y. ago) is characterized by intense bombardment, resetting of the geologic clocks, and excavation of the major basins such as Imbrium, Tranquillitatis, Serenitatis, Nectaris, etc. (refs. 94 and 100).
3. During the episode of mare flooding (3.9 to 3.16 b.y. ago), the basins

formed were filled with mare basalts. The ages of these lunar basalts are well documented by dating samples from the Apollo 11, 12, 15, and 17 and Luna 16 missions (refs. 18, 92, 93, 101 through 104, and others).

The failure to discover lunar igneous rocks younger than about 3.16 b.y. is an extremely important constraint in the lunar thermal history. Since basalts were probably derived from sources to about 400 km depth, the termination of lunar magmatic activity represents the end of melting or partial melting in the upper mantle of the Moon.

During the past 3.0 b.y., the lunar surface has continued to evolve as a result of meteorite impacts and cratering. There have been local melting and metamorphism in this period. There is no direct evidence for extensive volcanic activity or basalt flooding in the past 3.0 b.y.

Magnetism of Lunar Rocks

Although the Moon does not have a measurable dipole magnetic field at present, the lunar crust is extensively magnetized. This

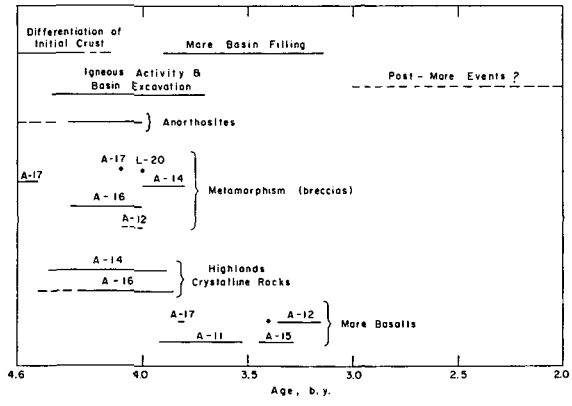

Figure 6.—*A summary of early lunar evolution and igneous activity at the surface, based on Rb-Sr, Ar^{39}-Ar^{40}, and concordia ages of returned lunar samples. Samples from different missions are designated by "A" for Apollo (A–11 is Apollo 11) and "L" for Luna. Sources for this summary are presented in the text.*

remanent magnetization has been verified by magnetic field measurements from the orbiting Apollo subsatellites (ref. 105), on the surface (ref. 71), and from the remanent magnetization of returned lunar samples (refs. 106 through 109, and others). This stable remanent magnetization was most likely acquired on the Moon as the rocks cooled through the Curie point of iron in the presence of a magnetic field. The intensity of the ambient magnetic field at the time of the formation of these rocks is estimated to be greater than 1000 gammas, and probably as high as a few thousand gammas (ref. 110).

The origin of the ancient magnetic fields which magnetized the initial lunar crust and the lunar rocks is one of the most important and as yet unresolved problems in lunar studies. From the ages of the crust and the rocks, the magnetizing field must have been present at least from 4.6 to 3.2 b.y. ago. The hypothesis of an external magnetizing field is not favored because of the difficulties associated with having a steady field of 1000 gammas or more near the Moon for a period of 1.5 b.y.

The favored hypothesis of the internally generated magnetizing field would require either a lunar dynamo or magnetized lunar interior (refs. 111, 112, and 113). In the dynamo model, it is necessary for the Moon to have a conducting iron or Fe/FeS core of sufficient size early in its history. The formation of such a molten core requires high internal temperatures early in the lunar history. In the case of a highly magnetized model of the lunar interior (refs. 111 and 113), it is required that the temperatures below a few hundred kilometers depth remain below the Curie temperature (about 760°C), while all the magmatic activity and differentiation take place at shallower depths. Such a model would put severe requirements on the thermal evolution models and also require a high magnetizing field at the time of the lunar accretion.

Thus, the magnetic history of the Moon according to the above models would require either extensive melting and differentiation

of the core at the onset of lunar evolution or temperatures less than about 800°C for the first 1.5 b.y. in the lunar mantle.

TEMPERATURE MODELS FOR THE MOON

In this section we present several specific models for the thermal evolution of the Moon which illustrate the effect of varying initial conditions and bulk radioactivities. Previous papers (refs. 23, 30, and 86) have discussed many of the models presented here and have assessed their ability to satisfy the constraints listed in the previous section. In this section we divide the models into three subgroups: initially homogeneous, convective, and inhomogeneous models.

Initially Homogeneous Models

We begin by considering a rather unrealistic model: initially cold (T = 0°C everywhere). This is a valuable exercise in the respect that it provides a verification of the computational scheme. Figure 7 shows three present-day temperature profiles each for the given present-day bulk uranium concentrations. Clearly, none of the models shown here satisfies the constraint of near-surface melting in the first billion years of the Moon's history. In fact, the basalt solidus (dashed line) is not reached at any point in time in the lunar evolution. Furthermore, while reasonable uranium concentrations of greater than 37 ppb provide present-day melting in the lunar interior, these models cannot generate enough heat to satisfy the above constraint. Since radioactive decay alone cannot provide the heat necessary for early melting and differentiation, we must consider models with high initial temperatures.

In an earlier section it was stated that one might consider the effects of early heating by tidal dissipation and/or solar wind flux as the Sun passed through a T-Tauri stage by investigating an initially completely molten Moon. Such a model is shown

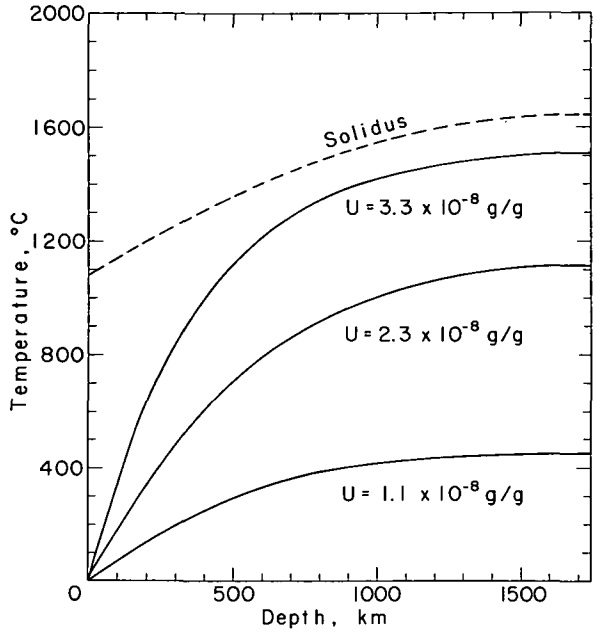

Figure 7.—*Present-day temperature profiles for an initially cold Moon (0°C everywhere), as a function of present-day uranium concentration. The solidus of anhydrous mare basalt (ref. 114) is also shown.*

in figure 8. In this case, all the radioactive heat sources are immediately differentiated and concentrated toward the surface. The formation of a dense core (ref. 86) composed of iron or FeS would easily be accomplished. Because of the depletion of heat sources in the lunar interior and the very effective heat transport in the convecting molten regions, this model cools rapidly and is completely solid after 2 b.y. At the present time it is completely solid and continuing to cool. With an average uranium composition of 60 ppb, the heat flow value is 29 erg/cm²-s, within the reported range of the Apollo 15 and 17 measurements. Although this model satisfies the constraints of early initial melting and heat flow, it does not allow for a small partially molten core as implied by the seismic data.

Since the normal process of accretion can produce initial near-surface partial melting without employing some catastrophic event, we now consider a model of lunar thermal evolution with initial temperatures calcu-

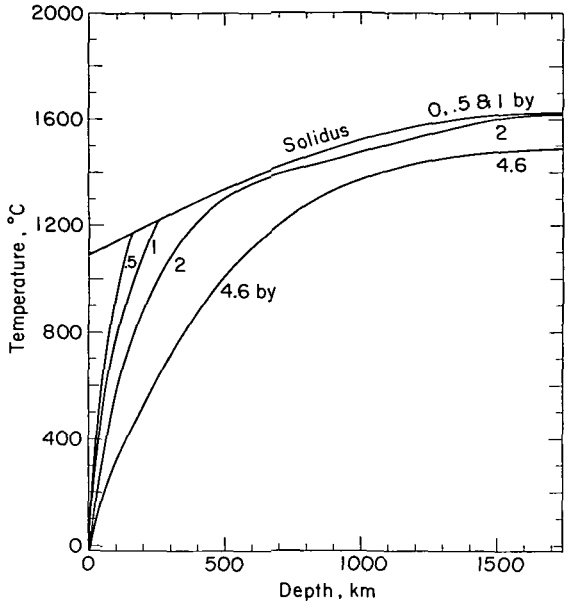

Figure 8.—*A model for thermal evolution as a function of time in an initially molten Moon. Time, in billions of years since lunar origin, is indicated by the number adjacent to each temperature profile. On this and later figures, the Moon is partially or completely molten at those depths where the temperature profile lies along the solidus.*

lated according to equations (1) and (2). This then allows for early segregation of the lunar crust and differentiation of the radioactive heat sources.

A model that satisfies all the major constraints presently known is shown in figure 9. The initial temperature is calculated from the accretion model, with an accretion time of 100 yr and a base temperature of 800°C, which allows for early heating by sources other than accretion. Initial melting extends to a depth of about 800 km, giving sufficient volume to differentiate a primordial lunar crust. The present-day uranium concentration averages to 60 ppb. The thermal conductivity is taken to be constant at 0.45×10^6 erg/cm-s-°C.

It can be seen from figure 9 that this model cools at the surface, giving a solid lithosphere growing at a rate of about 220 km per b.y. During the period of mare filling, the upper extent of melting progresses from 140 to 280 km, in agreement with the depth of origin of mare basalts (ref. 114) and with the necessity of maintaining a thick, cool lithosphere to sustain the stresses associated with mascon gravity anomalies. Shortly after 1 b.y., a convecting core develops due to undifferentiated heat sources of nearly primordial radioactive abundances near the center of the Moon. The core has a maximum radius of 1340 km at 1.5 b.y. and then slowly cools by conduction through the lithosphere. At present, this model is molten below 1000 km. This is in agreement with S-wave attenuation in the core region and with the occurrence of moonquakes at 700 to 800 km depth. The surface heat flow is 30 erg/cm^2-s, consistent with the measured values.

Convective Models

We now consider an approximation to solid-state convection in the Moon. We propose to simulate the efficient heat transport

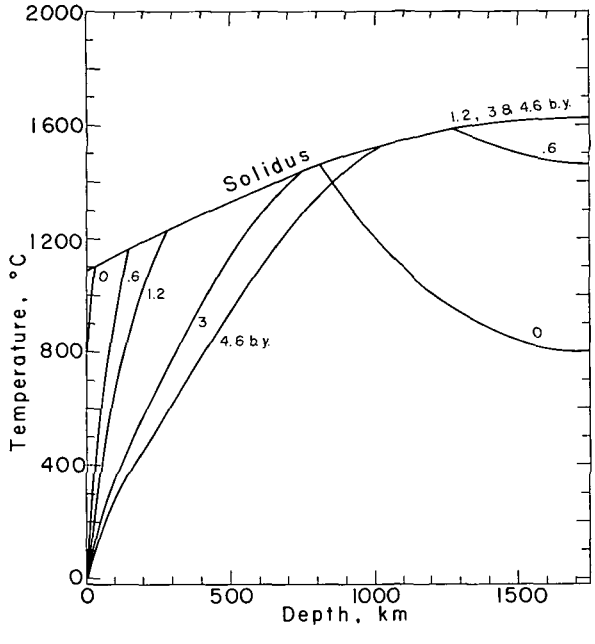

Figure 9.—*Thermal evolution in a Moon accreted in 100 yr at a base temperature of 800°C, with an average present-day uranium concentration of 60 ppb. Symbols are explained in the caption to figure 8.*

of convection by raising the thermal conductivity by a factor of 10 on a grid point that has a temperature greater than a critical temperature of 1000°C. This is equivalent to Tozer's steady-state "core" temperature. Otherwise, the conductivity follows the scheme of Schatz and Simmons (ref. 64). We permit this enhanced conduction after 1 b.y., i.e., after rapid differentiation is completed and a lithosphere has formed. As in the case of convection of molten material, this approximation does not include mass transport phenomena, nor is it a statement on any particular solid-state creep mechanism. It only enhances the heat transport.

Figure 10 illustrates a model with convection as described above. The initial conditions and present-day bulk uranium concentration are the same as for the previous model (fig. 9). The evolution proceeds as before until 1 b.y. At this point, convective processes dominate, and the conductivity is raised for temperatures above 1000°C. At the present, a convecting core of radius 1100 km and temperature nearly 1000°C underlies a nonconvecting, cool, rigid lithosphere. The present heat flow is 29 erg/cm²-s. The features of this model are essentially the same as Tozer's models.

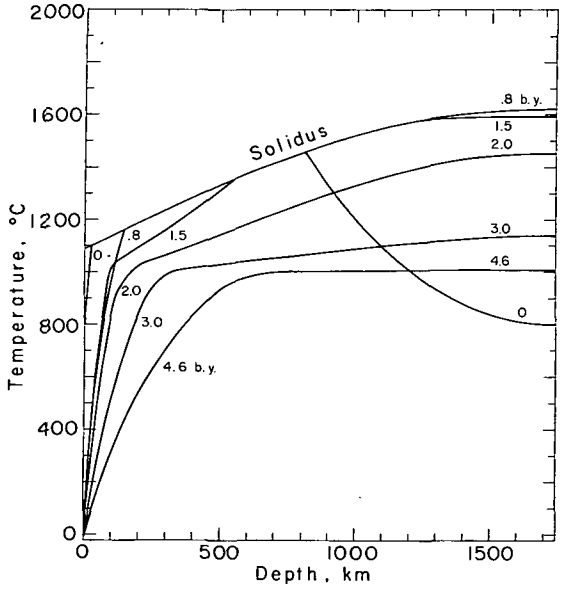

Figure 10.—*The effect of convection by solid state creep on the thermal evolution of the Moon (see text). The initial parameters for this model are the same as for figure 8.*

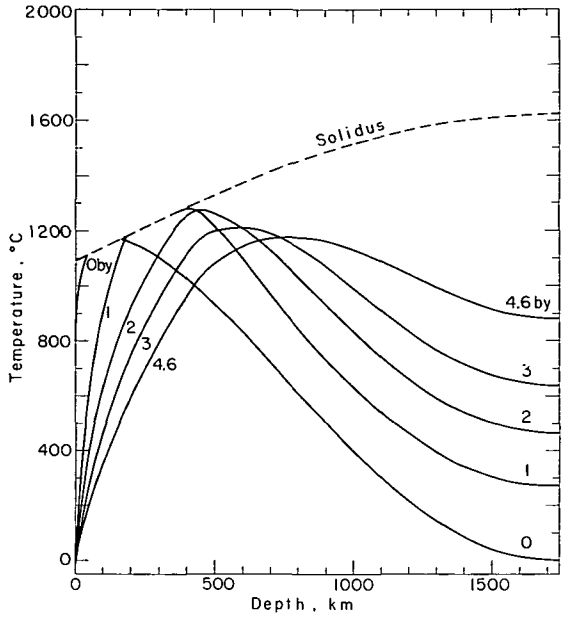

Figure 11.—*Thermal evolution in a Moon derived from inhomogeneous accretion (ref. 30). The initial temperature profile assumes a cold (0°C) accretion over a 1000-yr time interval. Primary zoning of radioactivity is assumed (see text).*

Inhomogeneous and "Blanketed" Models

We have considered up until this point models which assume an initially homogeneous distribution of heat sources in the Moon. The only exception was that of the molten Moon in which all the radioactive isotopes were initially differentiated to the surface. One type of model that allows relatively cool interior temperatures and satisfies the heat flow constraint without invoking solid-state convection has been suggested by several investigators (refs. 115, 116, and others). This involves a decrease in the concentration of radioactivity in the Moon, with depth as a primary feature associated with inhomogeneous accretion.

Figure 11 shoes a thermal history model

from Toksöz and Solomon (ref. 30) similar in many respects to the one proposed by McConnell and Gast (ref. 22). The initial temperature profile assumes accretion in 1000 yr, with a base temperature of 0°C. We assume that the radioactivity is stratified such that the present-day uranium abundance is 120 ppb in the uppermost 200 km, 50 ppb in the next 250 km, and 10 ppb in the remainder of the Moon. This gives a bulk uranium concentration of 53 ppb. The K/U and Th/U ratios are fixed with values given in table 1. The conductivity follows the Schatz and Simmons (ref. 64) model. Although the initial temperature barely exceeds the solidus between 40 and 140 km depth, shorter accretion times would provide initial melting at greater depths as in the previous models presented in this paper. With differentiation allowed for in four discrete time steps between 0 and 0.9 b.y., the evolution of the upper few hundred kilometers is similar to that in figures 9 and 10. The present-day heat flow is 32 erg/cm^2-s, and the interior of the Moon has temperatures well below the solidus.

The difference between this model and the others discussed earlier is that the interior of the Moon is depleted in radioactive elements at cold temperatures and, thus, heats slowly so that the Moon is everywhere solid at present. Whether or not a cold accretion can accompany primary chemical layering is debatable; however, such an origin is incompatible with a molten iron-rich core early in the Moon's history. Furthermore, as in the case of solid-state convection, the present-day temperature profile does not seem to satisfy the constraint implied by the attenuation of S-waves in the deep interior.

We finally examine the effect of a low thermal conductivity "blanket" layer on the Moon. Measurements of the effective thermal conductivity of uncompressed lunar soils (ref. 62) indicate values more than two orders of magnitude less than that assumed for the interior (see fig. 3). Some investigators have argued that the widespread distribution of these lunar fines following the large impact events 4 b.y. ago might have produced localized melting at shallow depths. Figure 12 compares such a model with that of figure 9, 100 m.y. after the soils are assumed to have been scattered. Since we are interested in the maximum possible effect of such an event, we will assume the lunar regolith to extend to a depth of 10 km, with a thermal conductivity of 0.45 $\times$ 10^4 erg/cm-s-°C. Both values are probably overestimates. The depth of dense fracturing in the lunar crust has been estimated to be less than 10 km by Toksöz et al. (ref. 80). Thermal conductivity increases rapidly with compression of the soils, and in-situ conductivity measurements made at the Apollo 15 and 17 heat flow sites (ref. 57) yield values only about 1 order of magnitude lower than the conductivity assumed for the bulk of the Moon. In any case, the maximum effect shown in figure 12 amounts to a rise in temperature of only about 180°C at 25 km. Thus, it can be confidently concluded that a uniform thermal "blanket" would have had

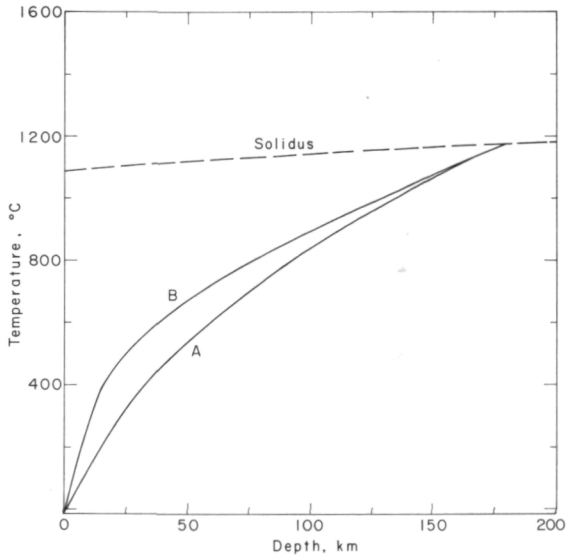

Figure 12.—*The maximum effect of a thermal "blanket" layer on near-surface lunar temperatures 100 m.y. after the presumed time of the Imbrium event (600 m.y. after lunar origin). Curve B represents a model with initial conditions the same as figure 9, but with the introduction of a low-conductivity, 10-km layer at 600 m.y. Curve A is the near-surface temperature profile for the model in figure 9, with no blanket layer.*

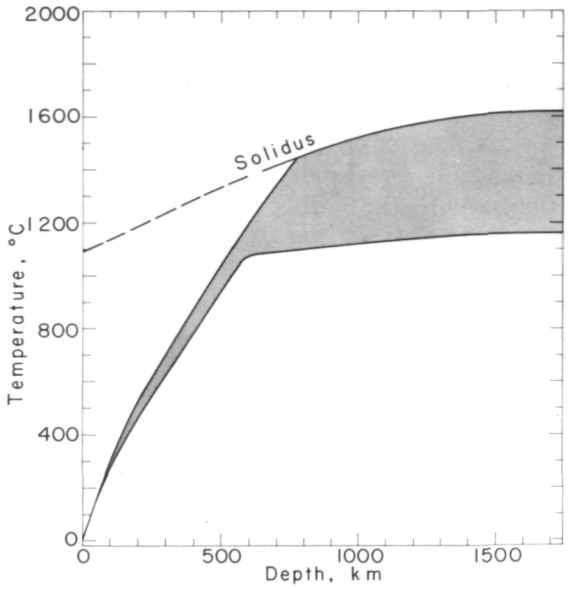

Figure 13.—*Range of present-day temperature profiles for theoretical thermal history calculations. The upper bound is from Toksöz and Solomon (ref. 30), while the lower bound is the convection solution of Turcotte et al. (ref. 66).*

a minimal effect on the early evolution of the Moon.

While the models discussed above are limited in number, they do serve to demonstrate the importance of initial conditions, geophysical constraints, and heat transport mechanisms in determining the thermal history of the Moon.

The range of present-day temperature profiles inside the Moon that satisfy the main constraints listed previously is shown in figure 13. One encouraging aspect of this figure is that regardless of how the temperatures are calculated, whether conduction or convection mechanisms are prevalent, the present-day temperatures are relatively narrow. Hopefully, with additional data, not only will the present-day temperature limits be narrowed, but also the early history of the Moon will be better understood.

EVOLUTION OF THE MOON

The thermal state of the lunar interior as a function of time is shown in figure 14, along with major episodes in lunar evolution. During the first 2 b.y., the lunar upper mantle undergoes sufficient melting to account for the differentiation of the crust and the subsequent lunar volcanism and mare filling. The zone of melting deepens with time. The lithosphere thickens at the rate of about 220 km/b.y. during this period. In particular, the shallowest melting progresses from 140 to 280 km depth during the period of mare filling, in agreement with the depth of origin of mare basalts (ref. 114) and with the need for a reasonably thick lithosphere to sustain the stresses associated with mascon gravity anomalies. The disappearance of melting in the mantle coincides roughly with the termination of magmatic events. At present the whole Moon is cooling. The deep interior, below a depth of 1000 km, may be hot enough for partial melting. This will explain the S-wave attenuation in this zone as described previously.

If indeed partially molten, the rheologic properties of the deep lunar interior may be

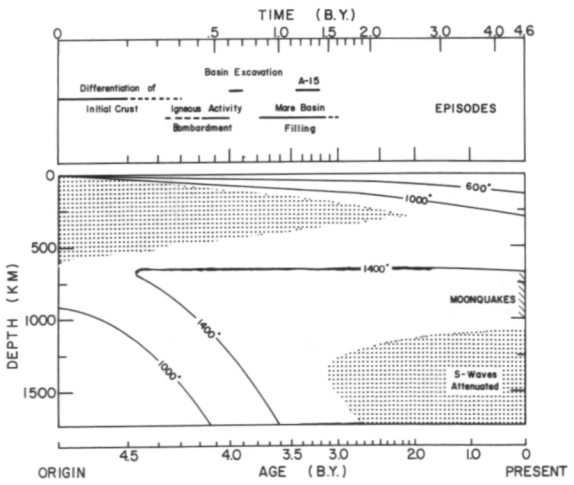

Figure 14.—*Thermal evolution of the lunar interior as a function of time, based on the temperature calculations shown in figure 9. Major episodes of differentiation and igneous activity are shown on top and are based on lunar sample ages. Isotherms are in 0° C. Fine and coarse shading denote regions of partial and extensive melting, respectively. Zones of moonquake activity and high attenuation of S-waves shown on the figure apply to the present.*

similar to the Earth's asthenosphere and may have convective motions. Such convection may exert small stresses at the bottom of the lithosphere where the moonquakes occur, but it could not induce sufficient stresses in the thick lunar lithosphere to cause large moonquakes or active tectonic motions.

Present-day temperatures shown in figure 13 and 14 generally exceed the melting temperatures of Fe or Fe/FeS combinations in the deep lunar interior. Thus, if there were a concentration of Fe or Fe/FeS in the center, it would be molten, and the Moon would have a molten core.

Thermal Evolution of Mars, Venus, and Mercury

In this section we calculate thermal history models for planets Mars, Venus, and Mercury. The Earth has been excluded from these calculations. Its evolution history is similar to that of Venus and is generally well understood. Its present-day temperatures are strongly constrained by the data, and models can be tailored to meet these requirements. New data that became available for Mars, Venus, and Mercury from recent planetary missions, however, justify a reexamination of the thermal histories of these planets.

For the calculations we use the numerical techniques described previously and follow a procedure similar to that used for the Moon. Since there are many fewer data for the planets, the calculated thermal models are less rigidly constrained than the lunar models.

MARS

The thermal history of Mars is not as strongly constrained as for the Moon or Earth. However, new data, primarily from the Martian Orbiter Mariner 9, provide information that places some conditions on its evolution and internal structure. We will now present several theoretically calculated thermal evolution models from Johnston et al. (ref. 32).

Structure and Constraints

The two main pieces of data regarding the composition and structure of the interior of Mars are its mass (M) and moment of inertia factor ($I/M\bar{R}^2$). These roughly determine the density variation within the planet and may indicate the presence (or absence) of a high-density core.

Using values of J_2 and the mean radius as determined from Mariner 9 experiments (ref. 117), we calculate $I/M\bar{R}^2 = 0.377 \pm 0.001$, indicating a distinct density increase with depth. This increase could easily be explained by a high-density core. Recent results from the U.S.S.R. Mars probe indicate that Mars maintains a relatively weak dipole magnetic field (ref. 118), giving further credence to the idea of a core.

The presence of a core places a fairly strong constraint on the thermal evolution. For core formation to take place, temperatures within the planet must have been nearly everywhere above a core material melting curve at one time. If Mars evolved in a manner similar to that of the Earth and Moon, the differentiation of core and mantle most likely took place relatively shortly after origin. It thus seems to be the case with Mars that volcanism and, therefore, differentiation have been active since early in the Martian history (ref. 119).

We assume that Mars has retained sulfur during its condensation and, thus, has an Fe-FeS core (refs. 58 and 120), and that potassium is partitioned into the sulphide phase (refs. 121 and 122), thus providing a heat source in the core by the decay of K^{40}. This model leads to early differentiation of Mars and early core formation, without requiring high initial temperatures necessary for the reduction of Fe or Si. This is possible due to the low and relatively pressure-independent Fe-FeS eutectic at 990°C (ref. 123).

Many new data concerning the evolution of Mars were obtained from the Mariner 9 photographs. The general picture was a planet much more dynamic than was previously thought. From the geologic interpre-

tation of these photographs (refs. 119, 124, 125, and 126), generally four regions of prominence stand out: an ancient cratered terrain, younger volcanic plains, large volcanic constructs such as shield volcanoes, domes, and craters, and extensive sedimentary deposits.

The Martian evolution inferred from the above features can be summarized as follows (ref. 126):

1. Roughly 4.6 b.y. ago Mars accreted. An intense bombardment of the surface took place at, or somewhat later than, the final stages, resulting in the heavily cratered, oldest terrain.
2. Volcanism, and probably the differentiation of the core, followed shortly thereafter.
3. Intense volcanic and tectonic activity characterized by basalt plains, uplifted, faulted, and eventually eroded, was apparently the next stage of Martian evolution. It was in this stage that the volcanic shields such as Nix Olympica began to develop.
4. The next stage featured large-scale tectonic activity and the completion of the shield volcanoes.
5. The final stage of evolution, lasting until the present, shows evidence of moderate tectonic and volcanic activity and wind and possibly water erosion and deposition.

Although no absolute ages are available for these stages of Martian evolution, they are valuable in constraining thermal history models. We know that an initial crust must have differentiated and the core formation must have occurred early in the Martian history, with volcanism, implying mantle melting, beginning shortly after and proceeding to the present time.

Heat Sources and Input Parameters

The thermal evolution models of Johnston et al. (ref. 32) are calculated in the manner described previously, with the exception that the formation of an Fe-FeS core and the differentiation of K^{40} into the core are specifically allowed.

As before, the most important heat source in the thermal history calculations is the heat generated by the decay of the long half-life radioactive isotopes U^{238}, U^{235}, Th^{232}, and K^{40}. No surface measurements of the abundances of these isotopes have been made for Mars, so we are forced to look at the only available data: those from the Earth, the Moon, and meterorites. The radioactive abundances for the Moon and some meteorites were discussed in an earlier section. The use of lunar, howarditic, or eucritic compositions in Mars, however, results in present-day temperatures too hot for any reasonable model.

The "chondritic coincidence" for the Earth has long been recognized (ref. 3), giving U = 11 ppb, but this requires the depletion of potassium in the crust relative to chondrites. Although putting the potassium in an Fe-FeS core can eliminate this problem, if all the excess potassium is put in the core, this increases the temperature significantly. In the other extreme, assuming no potassium in the core and K/U = 10 000, McDonald (ref. 7) recalculated the absolute uranium abundance for the Earth's mantle, constraining the heat production under steady-state conditions to match the average terrestrial heat flow. His uranium concentration, reduced to a homogeneous planet, is about 31 ppb. One might, therefore, place bounds on the Earth's absolute abundances, with U from 11 to 31 ppb and K/U from 80 000 to 10 000.

Recent models of the chemistry involved in the condensation of the solar nebula (refs. 59 and 127) indicate that a number of refractory trace elements, including the rare earths, will crystallize along with Ca-Al-rich assemblages at about 1500 K. This is before the condensation of magnesium silicates and metallic iron. Potassium and other volatiles will condense at lower temperatures (between 1100 K and 1200 K). Since these temperatures are higher than the condensation temperature for Mars ($\approx$ 450 K), we might expect that the planet retained solar propor-

tions of U, Th, and K. This amounts to a bulk uranium content of 15 ppb, with $K/U = 50\,000$ and $Th/U = 4$. We have assumed, however, a bulk radioactive abundance equivalent to MacDonald's Earth model; i.e., U = 31 ppb, and $K/U = 10\,000$. It is important to note, however, that the total heat production of these abundances is the same as that obtained with solar proportions. The only difference in the thermal modeling arises in the percentage of potassium allowed to enter the sulphide phase of the core. For solar abundances, this necessarily requires less potassium than is assumed in this paper (to be discussed later), but since little is know quantitatively about the partitioning of potassium, and given uncertainties in solar abundances, we believe this to be a minor effect.

The thermal conductivity of the Martian mantle is assumed to be temperature-dependent and described by the empirical equation derived by Schatz and Simmons (ref. 64). The silicate melting curve is taken to be an extrapolated peridotite solidus (ref. 128). Melting, convection of molten material, and differentiation of the radioactive isotopes are modeled as before.

The formation of the Fe-FeS core begins when temperatures in some portion of Mars exceed the Fe-FeS eutectic of 990°C and is completed when the temperatures for the bulk of the planet are above the liquidus for an assumed composition of iron and sulfur. In the calculations, core formation is modeled as both a continuous and discrete event. When the temperatures exceed the eutectic at a grid point, a small amount of excess heat, equivalent to the mass fraction of core material, is diverted to the next lower grid point and converted to its temperature equivalent. Thus, the core material effectively melts its way into the interior. Also, a specified percentage of the available potassium is released from the silicates in one discrete step and allowed to enter the core. Internal heating is also slightly enhanced by the gravitational settling of the molten metal. The temperature field is reset to an adiabatic gradient when the internal temperature rises above the Fe-FeS liquidus where it is believed sufficient mass transfer has occurred to warrant this action. The gravitational separation of the core is irreversible, and, once formed, the core does not react with the mantle.

We have assumed that the Fe-FeS eutectic and liquidus are unaffected by high-pressure phase changes of FeS. While this is apparently not the case (ref. 129), we maintain that the thermal models and conclusions presented in this paper remain essentially unchanged.

Parameters used in the thermal calculations may be found in table 1.

Thermal Models

Figure 15, taken from Johnston et al. (ref. 32), shows the effect of varying uranium concentrations. In the figure, the present-day temperatures in a uniform, initially cold ($T = 0°C$ everywhere) Mars are shown as a function of the present-day concentration of uranium. The terrestrial value of $K/U = 10\,000$ is assumed. Also shown are the Fe-FeS eutectic, the Fe-FeS liquidus for 85 wt%

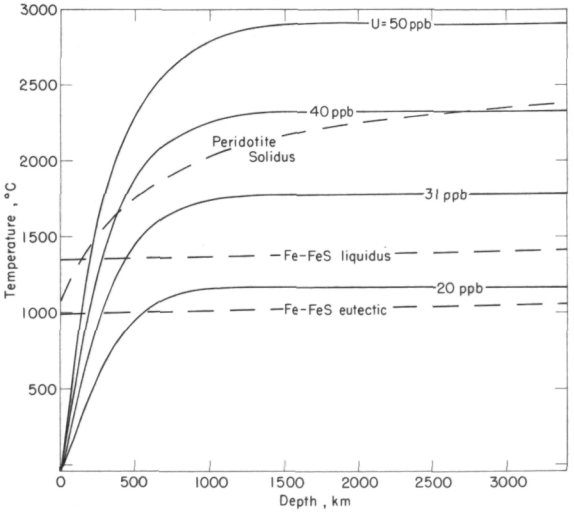

Figure 15.—*Present-day temperatures for an initially cold (0° C) Mars, as a function of uranium concentration. Also shown are the Fe-FeS eutectic and liquidus and the extrapolated peridotite solidus used in this paper (ref. 32).*

Fe, and the extrapolated peridotite solidus. No melting or differentiation is allowed. For $U \leq 37$ ppb, the temperatures are below the solidus. Clearly, these models do not satisfy the boundary condition that melting and differentiation of the silicates has occurred. For $U = 20$ ppb, the temperatures do not even exceed the Fe-FeS liquidus, prohibiting the completion of a core. To satisfy the boundary conditions, with the assumed radioactive heat production, higher initial temperatures must be used.

A thermal model that satisfies the major constraints on the evolution of Mars is shown in figure 16 (model "B" of ref. 32). The initial temperature is calculated from the accretion model, with an accretion time, τ, of 10^5 yr and a base temperature of 500°C. The core begins to form immediately and is completely formed by 1.0 b.y. Dry silicates begin to melt at 2 b.y. This zone of partial melt expands and works its way into the interior. The surface cools slowly by conduction, so that at the present time the dry solidus is reached at a depth of 1800 km. The calculated heat flow for this model is 43 erg/cm²-s, which is between the average measured heat flows for the Earth and Moon. The core is presently molten.

The evolution of Mars and the extent of melting is shown schematically for this model

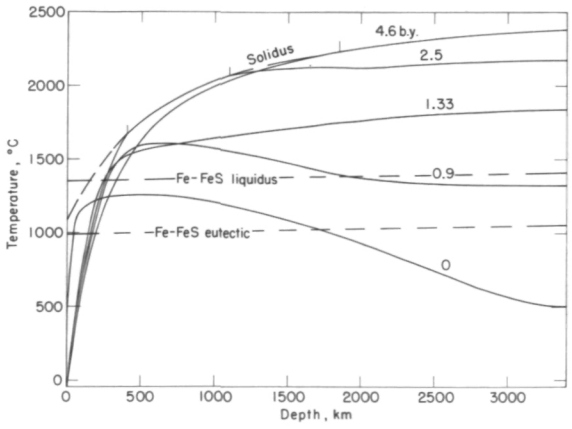

Figure 16.—*Thermal evolution of a Mars accreted in 10^5 yr, with T^b = 500°C. U = 31 ppb, with K/U = 10 000 (ref. 32).*

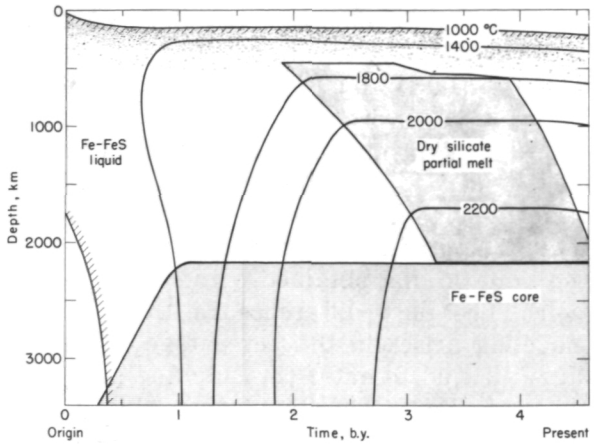

Figure 17.—*The evolution of the Martian interior as a function of time, based on the temperature calculations shown in figure 16. Isotherms are in ° C. The light shading above the dry silicate partial melt indicates the region where a small partial pressure of water would result in partial melt.*

in figure 17. Temperature and melting are plotted as functions of depth and time since origin. The light shading above the dry silicate melt shows regions where the introduction of a small partial pressure of water would result in a partial melt. Two episodes of Martian evolution are apparent from the figure. The first is the early differentiation of a crust due to partial melting in the near-surface regions and the formation of an Fe-FeS core. The formation of the crust is crucial in the understanding of the surface geology. Early volcanism, evident from Mariner photographs and the age of many regions inferred from crater densities, implies the formation and maintenance of a crust early in the Martian history. This is followed by upper mantle melting and differentiation probably resulting in extensive surface volcanism. The region of mantle partial melt progresses toward the interior as the surface slowly cools by conduction.

The presence of water and its relation to present-day tectonic activity is discussed in Johnston et al. (ref. 32). It was found that even for models such as the one discussed in this paper, where the anhydrous solidus is not reached until a depth of 1800 km, par-

tial melting can occur in the upper mantle. It is therefore concluded that one could expect moderate tectonic activity at the present time. A 200-km-thick lithosphere obtained for this model is consistent with the depth required by hydrostatics to elevate magma to the summit of volcanoes like Nix Olympica—about 23 km above the mean Martian sphere—and with the gravitational roughness of the planet.

Although the above temperature model is not a definitive statement about the present thermal state of Mars, it is adequate in the sense that all of the specified boundary conditions on thermal evolution are met. Hopefully, data from the future missions will provide additional constraints, and, thus, thermal models will be better specified.

VENUS

Venus is perhaps the most unconstrained planet as far as theoretically calculated thermal models are concerned. It can be supposed, however, that from size considerations alone, the evolution of Venus might be similar to the Earth's. There are, however, several important differences. Condensation models of the solar nebula imply that Venus retained little or no sulfur, thus eliminating the possibility of FeS or potassium in a core (ref. 58). Therefore, proceeding on the bias of early differentiation, we must require high initial temperatures in order to form a core within the first billion or so years. If one takes the moment of inertia factor for Venus to be equivalent to the Earth's (a rather strong assumption) it gives a core of radius about 2900 km for a composition of an Fe-Ni alloy. Lewis (ref. 58) also suggests that this core is surrounded by a massive mantle of Fe^{II}-free magnesium silicates. A crust, similar in composition to the Earth's, might also be expected.

Radar maps of the Venusian surface indicate relief of several kilometers (ref. 130). Considering the density and velocity of the atmosphere, we believe these features to be subject to extensive erosion and therefore young and probably of tectonic origin. Davidson and Anderson (ref. 131) have proposed that the rate of volcanism and tectonic activity is greater on Venus than on the Earth. Weertman (ref. 132), however, believes this not to be the case. Resolution of this conflict might be found from thermal models. Certainly, though, if the stresses associated with the nonhydrostatic state of Venus are not supported statically, we would have to expect convective motions in the upper mantle.

We now present a theoretical thermal model for Venus (fig. 18). The computational parameters for this model may be found in table 1. The initial temperature profile is calculated from equations (1) and (2), with an accretion time of 0.25×10^5 yr taken to ensure core differentiation within 1.0 b.y. The effect of adiabatic compression on the initial temperature is also included. The total heat production due to radioactive decay is essentially chondritic, having assumed uranium and potassium abundances equivalent to MacDonald's (ref. 7) Earth mantle values, i.e., U = 30 ppb, and K/U = 10 000 at the present day. This is consistent with theories on the condensation of the solar nebula (ref. 59). The bulk uranium concentration for

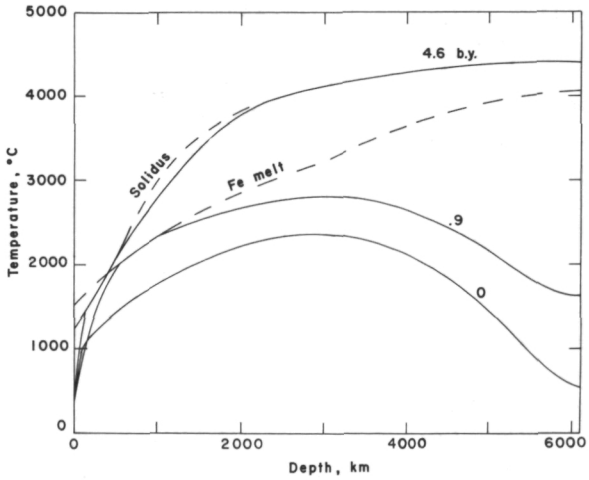

Figure 18.—*A model for the thermal evolution of Venus. The accretion time is 0.25 × 10⁵ yr, and the effect of compressional heating is included in the initial temperature. Input parameters for this model are described in the text.*

Venus might actually be slightly higher than the Earth's, due to the fact that it has not retained sulfur and, thus, has a lower mean atomic weight (ref. 58). The thermal conductivity of the undifferentiated planet and of the differentiated mantle is from the Schatz and Simmons (ref. 64) model.

Core formation is initiated when the temperatures within the interior exceed the Fe melting curve calculated for a homogeneous planet (ref. 133). At this point (about 1.0 b.y.), it is assumed that the rate of inflow of molten iron to the core is sufficient so that the gravitational energy due to core separation (refs. 134 and 135) allows for immediate core formation and temperatures in the interior are raised by the heat equivalent. We reset the temperature profile to an adiabatic gradient after core formation, due to the extensive mass transfer that has presumably taken place. Radioactive isotopes originally in the core region are displaced and distributed homogeneously throughout the mantle.

The temperature rise due to core infall is sufficient to initiate mantle melting immediately after core formation. The mantle melting curve is derived from Lindemann's equation which can be written in a form so that $T_m = \text{const}\ \phi$, where T_m is the melting temperature and ϕ is the seismic parameter (D. H. Chung, personal communication). Using measured values of ϕ for the Earth, this equation provides an adequate estimate for the mantle melting curve for Venus. Convection of molten material and differentiation of the radioactive isotopes are modeled as described previously.

Present-day temperatures are shown in the curve labeled 4.6 b.y. The iron melting curve shown in figure 18 is calculated for a differentiated planet. Notable features of this model are the thin (100-km) lithosphere, partially molten upper mantle, solid lower mantle, and molten core. Despite the molten core, the absence of a magnetic field for Venus can be explained by the lack of heat sources in the core and the slow rotation rate of the planet. Calculated heat flux is 98 ergs/cm^2-s.

Figure 19 shows schematically the evolution of Venus as a function of time. Isotherms are in degrees centigrade. As noted before, core formation takes place at 1.0 b.y., and present-day conditions indicate a region of high fractional partial melt (shaded area) in the upper mantle (higher than expected in the Earth), overlain by a lithosphere about 100 km thick. Although the degree of partial melt may be a function of the high surface temperature (presumably due to the atmosphere which may not have been in existence throughout the history of Venus), we have computed thermal models with the surface temperature arbitrarily set at 0°C. This results in a change of partial melt only in the upper few grid points. We therefore believe that any stresses associated with hydrostatic disequilibrium are supported within Venus by strong convective motions in the upper mantle. This points directly to the possibility of plate motion, similar to the Earth's and likely at a higher rate, and leads us to expect significant tectonic activity at the present time.

MERCURY

The knowledge of the planet Mercury has increased significantly since the Mariner 10 mission of April 1974. Preliminary results of television reconnaissance of the planet's

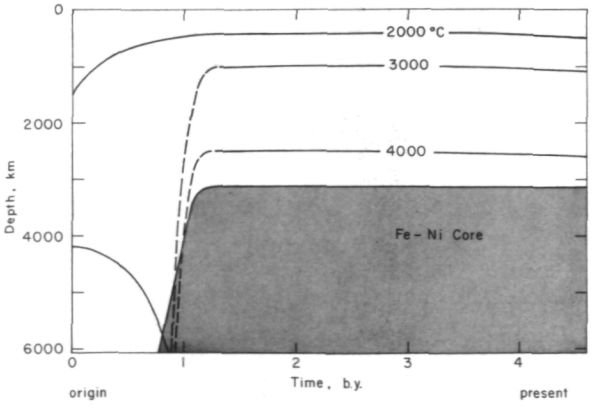

Figure 19.—*The evolution of Venus as a function of time, showing core formation and mantle melting (shaded region). Isotherms are in ° C.*

surface (ref. 136) show it to be remarkably similar to the lunar highlands. Regions resembling lunar mares have been observed, implying volcanic activity during Mercury's history. The presence of a magnetic field (ref. 137) could imply a molten iron core. We propose, then, that Mercury, as the other terrestrial planets, differentiated early, forming a crust similar to the Moon's and an iron core.

Siegfried and Solomon (ref. 33), using methods similar to those described earlier in this paper, have calculated several thermal and density models for Mercury. They point out, however, that Mercury is different from the other planets in the respect that condensation models of the solar nebula imply enrichment in refractory elements such as uranium and thorium and retention of little or no potassium and other volatiles. Furthermore, the thermal evolution is dominated by the high conductivity of iron, which makes up approximately 69 percent of the planet by weight.

Using appropriate initial temperatures, Siegfried and Solomon have shown that Mercury can indeed differentiate and form a core. Difficulties arise, however, if one assumes no heat source in the core and differentiation takes place earlier than about 3.0 b.y. These difficulties occur because the core is presently solid, with temperatures several hundred degrees lower than the iron melting curve calculated following Higgins and Kennedy (ref. 133). This is in apparent conflict with the presence of a magnetic field, if such a field is indeed due to an active core dynamo. Furthermore, differentiation at times earlier than 1.0 to 1.5 b.y. seems to be required from the nature of Mercury's surface.

We have therefore calculated a thermal model for Mercury (fig. 20), assuming the presence of some sort of heat source in the core. We have chosen this to be, as a matter of convenience, the decay of K^{40}. The initial temperature profile is calculated from the accretion model, with $\tau = 10^3$ yr, and $T_b = 1127°C$ (1400K), which provides initial iron melting to a depth of about 900 km. Thus, core formation and mantle melting are initiated immediately. Other model parameters such as uranium and thorium abundances are taken from Seigfried and Solomon (ref. 33) and may be found in table 1. Mantle conductivity is taken to be constant and equivalent to that used for the lunar thermal model presented in this paper ($K = 0.45 \times 10^6$ erg/cm-s °C).

As shown in figure 20, temperature profiles indicate a solid lithosphere 200 km thick at 2 b.y. and about 500 km thick at the present time. The core is presently partially molten and therefore might be able to sustain convective motions required to maintain a magnetic field. The lithosphere is probably thick enough to ensure a low level of tectonic activity. We would conclude from this model, however, that the regions on Mercury's surface that appear like the lunar mare may actually be younger, with tectonic activity having been prevalent on the planet for a longer period of time. We have also found that a K^{40} concentration of 0.156 ppm at the present time provides a minimum value required to maintain a partially molten core. The calculated heat flux is 60 ergs/cm^2-s.

For comparison we show a thermal model of Mercury in figure 21 that contains no heat source in the core. Other model parameters are the same as those described above. In this case, although the mantle and core differentiate, the entire planet has temperatures

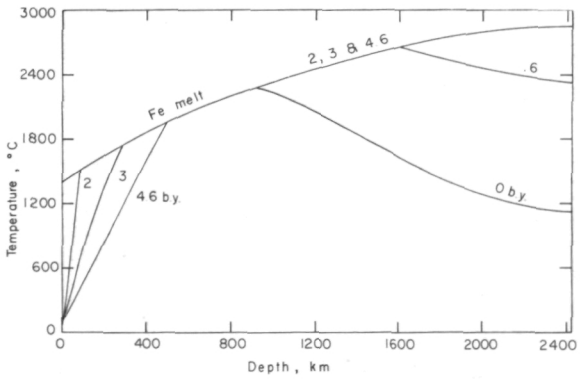

Figure 20.—*A thermal model of Mercury, with a heat source assumed in the core. Input parameters for this model are described in the text.*

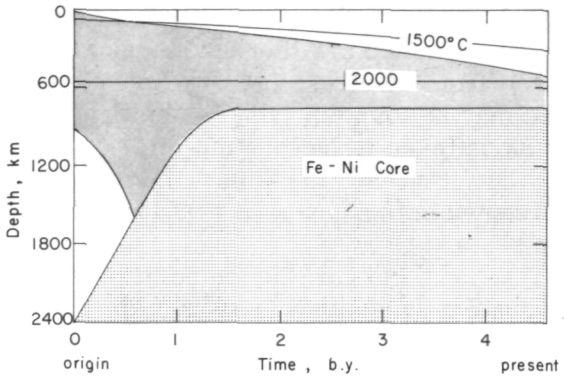

Figure 21.—*The thermal history of Mercury, with the same parameters as for the model in figure 20, except that the core is assumed to be free of heat sources.*

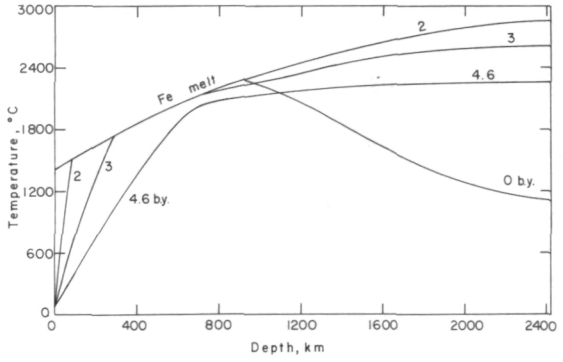

Figure 22.—*The evolution of Mercury as a function of time. Shading above the core region indicates mantle melting. Isotherms are in ° C.*

below the melting curve at the present time.

Figure 22 shows the evolution of Mercury as a function of time for the model in figure 20. Given the parameters used in this model, we conclude that Mercury could have a molten iron core if internal heat sources are assumed, and that present-day temperatures and the thickness of the lithosphere limit the tectonic activity to very low levels, if there is, in fact, any activitv.

Discussion and Conclusions

The thermal history models calculated for the Moon, Mars, Venus, and Mercury are representative of the whole spectrum of sizes and compositions of the terrestrial planets. The evolution histories are shown together in figure 23 for a comparative analysis. It is clear from this figure that although the initial temperatures are similar for these planets the evolution histories and present-day temperatures are quite different. The size (radius) of the planet more than any other factor seems to control its evolution and present-day thermal state. For the Moon and Mercury, the two smallest bodies, the evolution and differentiation took place relatively early in their histories. At present, both have thick lithospheres and are mostly solid. Venus, on the other hand, seems to be still at the peak of its evolution. Mars falls in between.

A good illustration of the comparison of evolutionary history of the planets can be obtained from the value of the total thermal energy of the planet as a function of time given by:

$$E(t) = (\int_v \rho C_p T(t)\,dV + Q(t))/M$$

where $E(t)$ is energy in ergs per gram, $T(t)$ the absolute temperature, and $Q(t)$ the heat that goes into fusion at time t. M is the mass, and V the volume of the planet. This is illustrated for the planets examined in this paper in figure 24.

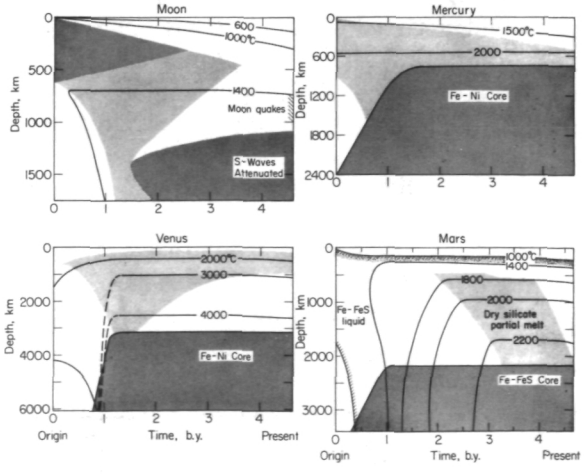

Figure 23.—*A comparison of the evolution of the planets.*

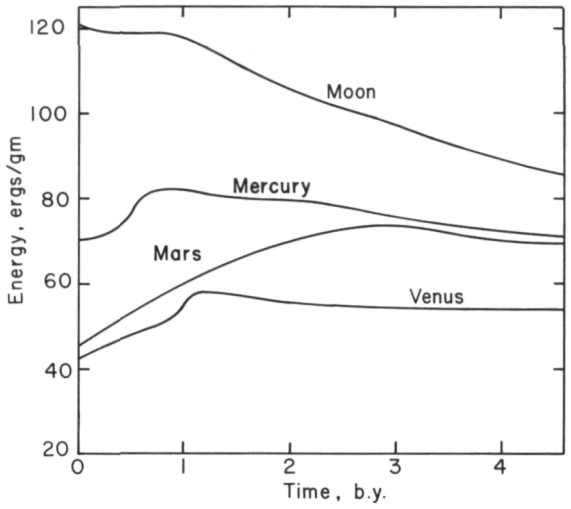

Figure 24.—*Total thermal energy as a function of time for the Moon, Mars, Mercury, and Venus.*

Several conclusions may be drawn from this figure. First, the maximum energy corresponds to the peak of the evolutionary process. Second, the rate of cooling is dependent primarily on the planet's size and somewhat on composition (that is, thermal conductivity).

For example, the Moon, which is the smallest planet, has a peak of thermal energy during the first billion years after formation. This corresponds roughly to the period of large-scale magmatic activity as evidenced by the mare basin filling. Afterwards, the energy level decreases rapidly as the Moon cools. At the present time we would expect the Moon to be relatively inactive tectonically. This is illustrated by a simple comparison with the Earth, which appears to be at the peak of its evolution at present. The terrestrial lithosphere is about 100 km thick, while that of the Moon is about 700 km. The Earth is tectonically active, with seismic energy release of about $E_s = 10^{25}$ ergs/yr, while the Moon is inactive with $E_s \simeq 10^{11}$ ergs/yr (ref. 90). While three-fourths of the Earth's surface is covered with rocks of 500 m.y. or younger, the youngest crystalline rock found on the Moon is 3.16 b.y.

Mercury, the next smallest planet, also reaches its peak of evolution early in its history. We would expect, upon examining figure 24 (with thermal energy calculated for the model shown in figure 20), that the bulk of the tectonic activity occurred before 2.0 b.y. The sharp increase in thermal energy is due to core formation. After 2.0 b.y. the energy decreases, showing that the planet is presently cooling and is probably dormant. If one does not include heat sources in the core, as in figure 21, the slope of $E(t)$ would be greater at the present time and the planet would obviously be cooler, heat transfer being dominated by the high conductivity of iron.

Mars, intermediate in size among the terrestrial planets, reached its peak of evolution around 3 b.y., maintained a relatively constant level of thermal energy for about a billion years, and is now beginning to cool. From this we can conclude that, while magmatic and tectonic activity have existed on Mars since early in its history, most of the volcanism and tectonics probably occurred in the last 2 b.y. We also expect a moderate level of tectonic activity at the present time.

Venus, in many respects similar to the Earth, differentiated a core early and has maintained a fairly constant level of thermal energy throughout its history. It can be considered to still be at its peak in evolution. Thus, we can expect tectonic processes in Venus similar to those observed on the Earth.

In interpreting the above results, one must be careful to note that the thermal energies calculated for each planet were taken from one nonunique thermal history model. These models, however, are reasonable in that they satisfy most of the constraints on the evolution of the planets known at the present time. Since they represent a bias toward early differentiation of all the terrestrial planets, the thermal energy turns out to be a useful tool to examine the effect of planetary size on the durations of high evolutionary and therefore tectonic activity.

In summary, we conclude the following:

1. The terrestrial planets were heated in some manner during or shortly after accretion.

2. This initial heating allowed for early core formation and/or differentiation. Early differentiation is evident from rock ages for the Earth and Moon and from photographic interpretation of Mars and Mercury surface features.
3. For planets with large cores such as the Earth, Venus, and Mercury, the energy released upon core separation is a large portion of the total heat budget of the planet.
4. The Moon is characterized as a differentiated body which evolved early in its history. The models that satisfy the constraints define a relatively narrow range for the temperatures in the outer several hundred kilometers, regardless of conduction and convective type calculations. Below 1000 km, the control on temperatures is not as great. Temperatures at the center of the Moon may be anywhere between 1000° and 1600°C. At these temperatures the Moon could have a partially molten (or, if Fe and FeS are differentiated, a totally molten) core.

   Acceptable evolution models require extensive differentiation and upward concentration of radioactive heat sources early in lunar history. This differentiation most likely is a product of extensive melting, although differentiation due to inhomogeneous accretion cannot be ruled out. A model of the Moon which is initially hot and extensively or totally molten can best satisfy the constraints.
5. Thermal models for Mars, assuming an Fe-FeS core composition, indicate formation of the core and the differentiation of an early crust within the first billion years after origin in order to satisfy the given constraints on the thermal evolution. These models involve large-scale differentiation of the mantle silicates in the past 2 b.y. This would be accompanied by volcanism and outgassing of volatiles at the surface. The inclusion of water in the upper mantle system leads to partial melting at a depth of about 22 km or greater at the present time.
6. Venus, while not as strongly constrained as the Moon or Mars, is characterized as a planet not unlike the Earth in many respects. Core formation is allowed to occur by 1.0 b.y., and present-day temperature profiles indicate a partially molten upper mantle overlain by a lithosphere approximately 100 km thick and a molten Fe-Ni core.
7. Mercury is taken to be similar to the Moon except for its large iron core. Thermal models with an assumed heat source in the core yield a planet that has a solid mantle to about 500 km depth, with a partially molten core. Those with no heat sources in the core have present-day temperatures well below the melting curve for iron, heat transfer being dominated by the high thermal conductivity of the iron.
8. The examination of total thermal energy as a function of time for each planet provides a method for determining the effect of planetary size on the durations of high tectonic activity. The Moon, smallest in size, is presently cool and tectonically inactive. Mercury is probably inactive at the present time, but its peak of activity lasted longer than the Moon's. Mars, intermediate in size, reached its peak in evolution in the past several billion years, but is probably moderately active at the present time. Venus, having been able to retain its thermal energy throughout its history, may today have tectonic processes similar to the Earth's.

Acknowledgment

The authors wish to thank Robert W. Siegfried and Dr. Sean C. Solomon for valuable discussions and the use of their computer program for Mercury and Eileen Schaffer for her contribution to the computations.

This research was supported by NASA grants NGL 22–009–187 and NSG–7081 (BASIC) and Contract No. 66437B under NASA Contract NAS1–9703.

References

1. UREY, H. C., The Origin and Development of the Earth and Other Terrestrial Planets. *Geochimica et Cosmochimica Acta*, Vol. 1, 1951, pp. 209–277.
2. UREY, H. C., *The Planets, Their Origin and Development*, Yale University Press, New Haven, Connecticut, 1952.
3. UREY, H. C., The Cosmic Abundances of Potassium, Uranium and Thorium and the Heat Balances of the Earth, Moon, and Mars. *Proc. Natl. Acad. Sci. U.S.*, Vol. 41, 1955, pp. 127–144.
4. UREY, H. C., Boundary Conditions for Theories of the Origin of the Solar System. *Physics and Chemistry of the Earth, 2*, L. H. Ahrens, F. Press, K. Rankama, and S. K. Runcorn, eds., Pergamon Press, New York, 1957, pp. 46–76.
5. UREY, H. C., Origin and History of the Moon. *Physics and Astronomy of the Moon, 1st Ed.*, Z. Kopal, ed., Academic Press, New York, 1962, p. 481.
6. LUBIMOVA, H., Thermal History of the Earth With Consideration of the Variable Thermal Conductivity of Its Mantle. *Geophys. J.*, Vol. 1, 1958, p. 115.
7. MACDONALD, G. J. F. Calculations on the Thermal History of the Earth. *J. Geophys. Res.*, Vol. 64, 1959, pp. 1967–2000.
8. MACDONALD, G. J. F., The Deep Structure of Continents. *Rev. Geophys.*, Vol. 1, 1963, p. 587.
9. LEVIN, B. J., Thermal History of the Moon. *The Moon*, Z. Kopal and Z. K. Mikhailov, eds., Academic Press, New York, 1962, p. 157.
10. ANDERSON, D. L., AND R. A. PHINNEY, Early Thermal History of the Terrestrial Planets. *Mantles of the Earth and Terrestrial Planets*, S. K. Runcorn, ed., Interscience, London, 1967, pp. 113–126.
11. FRICKER, P. E., R. T. REYNOLDS, AND A. L. SUMMERS, On the Thermal History of the Moon. *J. Geophys. Res.*, Vol. 72, 1967, p. 2649.
12. FRICKER, P. E., R. T. REYNOLDS, AND A. L. SUMMERS, On the Thermal Evolution of the Terrestrial Planets. *The Moon*, Vol. 9, 1974, pp. 211–218.
13. MCCONNELL, R. K., JR., L. A. MCCLAINE, D. W. LEE, J. R. ARONSON, AND R. V. ALLEN, A Model for Planetary Igneous Differentiation. *Rev. Geophys.*, Vol. 5, 1967, p. 121.
14. LEE, W. H. K., Effects of Selective Fusion on the Thermal History of the Moon, Mars, and Venus. *Earth Planet. Sci. Letters*, Vol. 4, 1968, p. 277.
15. HANKS, T. C., AND D. L. ANDERSON, The Early Thermal History of the Earth. *Phys. Earth Planet. Interiors*, Vol. 2, 1969, pp. 19–29.
16. MAJEVA, S. V., The Thermal History of the Terrestrial Planets. *Astrophys. Letters*, Vol. 4, 1969, p. 11.
17. UREY, H. C., AND G. J. F. MACDONALD, Origin and History of the Moon. *Physics and Astronomy of the Moon, 2nd Ed.*, Z. Kopal, ed., Academic Press, New York, 1971, pp. 213–289.
18. PAPANASTASSIOU, D. A., AND G. J. WASSERBURG, Lunar Chronology and Evolution From Rb-Sr Studies of Apollo 11 and 12 Samples. *Earth Planet. Sci. Letters*, Vol. 11, 1971, pp. 37–62.
19. HAYS, J. F., Radioactive Heat Sources in the Lunar Interior. *Phys. Earth Planet. Interiors*, Vol. 5, 1972, pp. 77–84.
20. WOOD, J. A., Thermal History and Early Magmatism in the Moon. *Icarus*, Vol. 16, 1972, pp. 229–240.
21. REYNOLDS, R. T., P. E. FRICKER, AND A. L. SUMMERS, Thermal History of the Moon. *Thermal Characteristics of the Moon*, J. W. Lucas, ed., MIT Press, Cambridge, 1972, pp. 303–337.
22. MCCONNELL, R. K., JR., AND P. W. GAST, Lunar Thermal History Revisited. *The Moon*, Vol. 5, 1972, pp. 41–51.
23. TOKSÖZ, M. N., S. C. SOLOMON, J. W. MINEAR, AND D. H. JOHNSTON, Thermal Evolution of the Moon. *The Moon*, Vol. 4, 1972, p. 190, and Vol. 5, 1972, p. 249.
24. TOZER, D. C., The Moon's Thermal State and an Interpretation of the Lunar Electrical Conductivity Distribution. *The Moon*, Vol. 5, 1972, pp. 90–105.
25. TOZER, D. C., The Present Thermal State of the Terrestrial Planets. *Phys. Earth Planet. Interiors*, Vol. 6, 1972, pp. 182–197.
26. TOZER, D. C., The Internal Evolution of Planetary Size Objects. *The Moon*, in press, 1973.
27. HANKS, T. C., AND D. L. ANDERSON, Origin, Evolution and Present Thermal State of the Moon. *Phys. Earth Planet. Interiors*, Vol. 5, 1972, pp. 409–425.
28. DUBA, A., AND A. E. RINGWOOD, Electrical Conductivity, Internal Temperatures and Thermal Evolution of the Moon. *The Moon*, Vol. 7, 1973, pp. 356–376.
29. CASSEN, P., AND R. T. REYNOLDS, The role of Convection in the Moon. *J. Geophys. Res.*, Vol. 78, 1973, pp. 3203–3215.
30. TOKSÖZ, M. N., AND S. C. SOLOMON, Thermal History and Evolution of the Moon. *The Moon*, Vol. 7, 1973, pp. 251–278.

31. TOKSÖZ, M. N., AND D. H. JOHNSTON, The Evolution of the Moon. *Icarus*, Vol. 21, in press, 1974.
32. JOHNSTON, D. H., T. R. MCGETCHIN, AND M. N. TOKSÖZ, The Thermal State and Internal Structure of Mars. *J. Geophys. Res.*, in press, 1974.
33. SIEGFRIED, R. W., AND S. C. SOLOMON, Mercury: Internal Structure and Thermal Evolution. *Icarus*, in press, 1974.
34. SCHUBERT, G., AND R. E. YOUNG, Internal Temperature of Mars. *EOS, Trans. Am. Geophys. Union*, Vol. 55, 1974, p. 343.
35. SCHRAMM, D. N., F. TERA, AND G. J. WASSERBURG, The Isotopic Abundance of Mg^{26} and Limits of Al^{26} in the Early Solar System. *Earth Planet. Sci. Letters*, Vol. 10, 1970, pp. 44–59.
36. FISH, R. A., G. G. GOLES, AND E. ANDERS, The Record of the Meteorites: III. On the Development of Meteorites in Asteroidal Bodies. *Astrophys. J.*, Vol. 132, 1960, pp. 143–256.
37. KAULA, W. M., Thermal Effects of Tidal Friction. *The Earth-Moon System*, B. G. Marsden and A. G. W. Cameron, eds., Plenum Press, New York, 1966, pp. 46–51.
38. SINGER, S. F., Origin of the Moon by Capture and Its Consequences. *EOS, Trans. Am. Geophys. Union*, Vol. 51, 1970, pp. 637–640.
39. HALLAM, M., Heat Sources for Early Differentiation of the Lunar Interior (abs.). *EOS, Trans. Am. Geophys. Union*, Vol. 54, 1973, p. 344.
40. SONETT, C. P., AND D. S. COLBURN, The Role of Accretionally and Electrically Inverted Thermal Profiles in Lunar Evolution. *The Moon*, Vol. 1, 1970, pp. 483–484.
41. MIZUTANI, H., T. MATSUI, AND H. TAKEUCHI, Accretion Process of the Moon. *The Moon*, Vol. 4, 1972, pp. 476–489.
42. LSPET (Lunar Sample Preliminary Examination Team), *Science*, Vol. 175, 1972, p. 363.
43. LSPET (Lunar Sample Preliminary Examination Team), *Science*, Vol. 179, 1973, p. 23.
44. O'KELLEY, G. D., J. S. ELDRIDGE, E. SCHONFELD, AND P. R. BELL, Primordial Radionuclide Abundances, Solar Proton and Cosmic-Ray Effects and Ages of Apollo 11 Lunar Samples by Non-Destructive Gamma Ray Spectrometry. *Proc. Apollo 11 Lunar Science Conference*, Vol. 2, A. A. Levinson, ed., 1970, pp. 1403–1423.
45. CLARK, R. S., AND J. E. KEITH, Determination of Natural and Cosmic Ray Induced Radionuclides in Apollo 16 Lunar Samples. *Proc. Fourth Lunar Science Conference (abs.)*, 1973, pp. 146–147.
46. SILVER, L. T., Uranium-Thorium-Lead Isotopic Characteristics. *Proc. Fourth Lunar Science Conference (abs.)*, 1973, pp. 673–674.
47. TATSUMOTO, M., P. D. NUMES, AND R. J. KNIGHT, U-Th-Pb Systematics of Some Apollo 16 Samples. *Proc. Fourth Lunar Science Conference (abs.)*, 1973, pp. 705–707.
48. PERKINS, R. W., L. A. RANCITELLI, J. A. COOPER, J. H. KAYE, AND N. A. WOGMAN, Cosmogenic and Primordial Radionuclide Measurements in Apollo 11 Lunar Samples by Nondestructive Analysis. *Proc. Apollo 11 Lunar Science Conference*, Vol. 2, A. A. Levinson, ed., 1970, pp. 1455–1469.
49. METZGER, A. E., J. I. TROMBKA, L. E. PETERSON, R. C. REEDY, AND J. R. ARNOLD, A First Look at the Lunar Orbital Gamma-Ray Data. *Proc. Third Lunar Science Conference*, Vol. 3, D. R. Criswell, ed., frontispiece, 1972.
50. PAPANASTASSIOU, D. A., AND G. J. WASSERBURG, Rb-Sr Ages of Igneous Rocks From the Apollo 14 Mission and the Age of the Fra Mauro Formation. *Earth Planet. Sci. Letters*, Vol. 12, 1971, pp. 36–48.
51. MASON, B., *Handbook of Elemental Abundances in Meteorites*, Gordon and Breach, New York, 1971.
52. LSPET (Lunar Sample Preliminary Examination Team), *Science*, Vol. 165, 1969, p. 1211.
53. DUKE, M. B., AND L. T. SILVER, Petrology of Eucrites, Howardites and Mesosiderites. *Geochimica et Cosmochimica Acta*, Vol. 31, 1967, pp. 1637–1665.
54. ANDERSON, D. L., The Composition and Origin of the Moon. *Earth Planet. Sci. Letters*, Vol. 18, 1973, pp. 301–316.
55. WÄNKE, H., H. BADDENHAUSEN, G. DREIBUS, M. QUIJANO-RICO, H. PALME, B. SPETTEL, AND F. TESCHKE, Multielement Analysis of Apollo 16 Samples and About the Composition of the Whole Moon. *Lunar Science*, Vol. IV, J. W. Chamberlain and C. Watkins, eds., Lunar Science Institute, Houston, 1973, pp. 761–763 and 767–769.
56. LANGSETH, M. G., JR., S. P. CLARK, JR., J. L. CHUTE, JR., S. J. KEIHM, AND A. E. WECHSLER, The Apollo 15 Lunar Heat-Flow Measurement. *The Moon*, Vol. 4, 1972, pp. 390–410.
57. LANGSETH, M. G., J. L. CHUTE, AND S. KEIHM, Direct Measurements of Heat Flow From the Moon. *Lunar Science*, Vol. IV, J. W. Chamberlain and C. Watkins, eds., Lunar Science Institute, Houston, 1973, pp. 455–456.
58. LEWIS, J. S., Metal/Silicate Fractionation in the Solar System. *Earth Planet. Sci. Letters*, Vol. 15, 1972, p. 286.
59. GROSSMAN, L., and J. W. LARIMER, Early Chemical History of the Solar System. *Rev. Geophys. and Space Phys.*, Vol. 12, 1974, p. 71.
60. CLARK, S. P., JR., Handbook of Physical Constants. *Geol. Soc. Am. Memoir 97*, 1966.
61. LACHENBRUCH, A. H., Preliminary Geothermal

Model of the Sierra Nevada. *J. Geophys. Res.*, Vol. 73, 1968, p. 6977.

62. CREMERS, C. J., Density, Pressure and Temperature Effects on Heat Transfer in Lunar Material. *AIAA J.*, Vol. 9, 1971, p. 2180.
63. HORAI, K., G. SIMMONS, H. KANAMORI, AND D. WONES, Thermal Diffusivity, Conductivity and Thermal Inertia of Apollo 11 Lunar Material. *Proc. Apollo 11 Lunar Science Conference*, Vol. 3, A. A. Levinson, ed., 1970, pp. 2243–2249.
64. SCHATZ, J. F., AND G. SIMMONS, Thermal Conductivity of Earth Materials at High Temperatures. *J. Geophys. Res.*, Vol. 77, 1972, pp. 6966–6983.
65. REYNOLDS, R. T., P. E. FRICKER, AND A. L. SUMMERS, Effects of Melting Upon Thermal Models of the Earth. *J. Geophys. Res.*, Vol. 71, 1966, pp. 573–582.
66. TURCOTTE, D. L., A. J. HSUI, K. E. TORRANCE, AND E. R. OXBURGH, Thermal Structure of the Moon. *J. Geophys. Res.*, Vol. 77, 1972, pp. 6931–6939.
67. CASSEN, P., AND R. T. REYNOLDS, *Convection in the Moon: Effect of Variable Viscosity.* In press, 1973.
68. SCHUBERT, G., D. L. TURCOTTE, AND E. R. OXBURGH, Stability of Planetary Interiors. *Geophys. J. R. Astr. Soc.*, Vol. 18, 1969, p. 441.
69. RUNCORN, S. K., Convection in the Moon. *Nature*, Vol. 195, 1962, pp. 1150–1151.
70. RUNCORN, S. K., Convection in the Moon and the Existence of a Lunar Core. *Proc. Roy. Soc. London, Ser. A*, Vol. 296, 1967, pp. 270–284.
71. DYAL, P., C. W. PARKIN, and P. CASSEN, Surface Magnetometer Experiments: Internal Lunar Properties and Lunar Field Interactions With the Solar Plasma. *Proc. Third Lunar Science Conference*, Vol. 3, D. R. Criswell, ed., 1972, pp. 2287–2307.
72. DYAL, P., C. W. PARKIN, AND W. D. DAILY, Surface Magnetometer Experiments: Internal Lunar Conductivity Profile and Steady Field Measurements. *Lunar Science*, Vol. IV, J. W. Chamberlain and C. Watkins, eds., Lunar Science Institute, Houston, 1973, p. 205.
73. SONETT, C. P., D. S. COLBURN, P. DYAL, C. W. PARKIN, B. F. SMITH, G. SCHUBERT, AND K. SCHWARTZ, Lunar Electrical Conductivity Profile. *Nature*, Vol. 230, 1971, pp. 359–362.
74. SONETT, C. P., B. F. SMITH, D. S. COLBURN, AND K. SCHWARTZ, The Induced Magnetic Field of the Moon: Conductivity Profiles and Inferred Temperature. *Proc. Third Lunar Science Conference*, Vol. 3, D. R. Criswell, ed., 1972, pp. 2309–2336.
75. HOUSLEY, R. M., AND F. J. MORIN, Electrical Conductivity of Olivine and the Lunar Temperature Profile. *The Moon*, Vol. 4, 1972, pp. 35–38.
76. OLHOEFT, G. R., A. L. FRISILLO, D. W. STRANGWAY, AND H. SHARPE, Electrical Properties of Lunar Solid Samples. *Lunar Science*, Vol. IV, J. W. Chamberlain and C. Watkins, eds., Lunar Science Institute, Houston, 1973, p. 575.
77. ANDERSON, D. L., AND T. C. HANKS, Is the Moon Hot or Cold? *Science*, Vol. 178, 1972, pp. 1245–1249.
78. TOKSÖZ, M. N., F. PRESS, K. ANDERSON, A. DAINTY, G. LATHAM, M. EWING, J. DORMAN, D. LAMMLEIN, G. SUTTON, F. DUENNEBIER, AND Y. NAKAMURA, Lunar Crust: Structure and Composition. *Science*, Vol. 176, 1972, pp. 1012–1016.
79. TOKSÖZ, M. N., F. PRESS, A. DAINTY, K. ANDERSON, G. LATHAM, M. EWING, J. DORMAN, D. LAMMLEIN, G. SUTTON, AND F. DUENNEBIER, Structure, Composition and Properties of Lunar Crust. *Proc. Third Lunar Science Conference*, Vol. 3, D. R. Criswell, ed., 1972, pp. 2527–2544.
80. TOKSÖZ, M. N., A. M. DAINTY, S. C. SOLOMON, AND K. R. ANDERSON, Velocity Structure and Evolution of the Moon. *Lunar Science*, Vol. IV, J. W. Chamberlain and C. Watkins, eds., Lunar Science Institute, Houston, 1973, pp. 734–736.
81. NAKAMURA, Y., G. LATHAM, D. LAMMLEIN, M. EWING, F. DUENNEBIER, AND J. DORMAN, Deep Lunar Interior Inferred From Recent Seismic Data. *Geophys.*, 1974.
82. TOKSÖZ, M. N., A. M. DAINTY, S. C. SOLOMON, AND K. R. ANDERSON, Structure of the Moon. *Rev. Geophys. and Space Phys.*, in press, 1974.
83. LATHAM, G., J. DORMAN, F. DUENNEBIER, M. EWING, D. LAMMLEIN, AND Y. NAKAMURA, Moonquakes, Meteoroids and the State of the Lunar Interior. *Lunar Science*, Vol. IV, J. W. Chamberlain and C. Watkins, eds., Lunar Science Institute, Houston, 1973, pp. 457–459.
84. NAKAMURA, Y., D. LAMMLEIN, G. LATHAM, M. EWING, J. DORMAN, F. PRESS, AND M. N. TOKSÖZ, New Seismic Data on the State of the Deep Lunar Interior. *Science*, Vol. 181, 1973, p. 49.
85. SOLOMON, S. C., Density Within the Moon and Implications for Lunar Composition. *The Moon*, in press, 1973.
86. SOLOMON, S. C., AND M. N. TOKSÖZ, Internal Constitution and Evolution of the Moon. *Phys. Earth Planet. Interiors*, Vol. 7, 1973, pp. 15–38.
87. BALDWIN, R. B., Absolute Ages of the Lunar Maria and Large Craters: II. The Viscosity of the Moon's Outer Layers. *Icarus*, Vol. 13, 1970, pp. 215–225.
88. ARKANI-HAMED, J., Viscosity of the Moon: I.

After Mare Formation. *The Moon*, Vol. 6, 1973, pp. 100–111.

89. LATHAM, G., M. EWING, J. DORMAN, D. LAMMLEIN, F. PRESS, M. N. TOKSÖZ, G. SUTTON, F. DUENNEBIER, AND Y. NAKAMURA, Moonquakes and Lunar Tectonism. *The Moon*, Vol. 4, 1972, pp. 373–382.
90. LAMMLEIN, D., G. LATHAM, J. DORMAN, Y. NAKAMURA, AND M. EWING, Lunar Seismicity, Structure and Tectonics. *Rev. Geophys. and Space Phys.*, in press, 1973.
91. SILVER, L. T., Uranium-Thorium-Lead Isotopes in Some Tranquillity Base Samples and Their Implications for Lunar History. *Proc. Apollo 11 Lunar Science Conference*, Vol. 2, A. A. Levinson, ed., 1970, pp. 1533–1574.
92. WASSERBURG, G. J., AND D. A. PAPANASTASSIOU, Age of an Apollo 15 Mare Basalt; Lunar Crust and Mantle Evolution. *Earth Planet. Sci. Letters*, Vol. 13, 1971, pp. 97–104.
93. TATSUMOTO, M., C. E. HEDGE, B. R. DOE, AND D. M. UNRUH, U-Th-Pb and Rb-Sr Measurements on Some Apollo 14 Lunar Samples. *Proc. Third Lunar Science Conference*, Vol. 2, D. Heymann, ed., 1972, pp. 1531–1555.
94. TERA, F., D. A. PAPANASTASSIOU, AND G. J. WASSERBURG, A Lunar Cataclysm at ~3.95 ae and the Structure of the Lunar Crust. *Lunar Science*, Vol. IV, J. W. Chamberlain and C. Watkins, eds., Lunar Science Institute, Houston, 1973, pp. 723–725.
95. ALBEE, A. L., A. A. CHODOS, R. F. DYMEK, A. J. GANCARZ, D. S. GOLDMAN, D. A. PAPANASTASSIOU, AND G. J. WASSERBURG, Dunite From the Lunar Highlands: Petrography, Deformational History, Rb-Sr Age. *Lunar Science*, Vol. V, Lunar Science Institute, Houston, 1974, p. 3.
96. WOOD, J. A., J. S. DICKEY, JR., U. B. MARVIN, AND B. N. POWELL, Lunar Anorthosites. *Science*, Vol. 167, 1970, p. 602.
97. DOE, B., Lunar Chronology. Written Communication, 1973.
98. HUSAIN, L., O. A. SCHAEFFER, AND J. F. SUTTER, Age of a Lunar Anorthosite. *Science*, Vol. 175, 1972, pp. 428–430.
99. SCHONFELD, E., AND C. MEYER, JR., The Abundances of Components of the Lunar Soils by a Least Squares Mixing Model and the Formation Age of KREEP. *Proc. Third Lunar Science Conference*, Vol. 2, D. Heymann, ed., 1972, pp. 1397–1420.
100. TERA, F., AND G. J. WASSERBURG, Lead Isotopic Evidence on Lunar Evolution. *EOS, Trans. Am. Geophys. Union*, Vol. 54, 1973, p. 355.
101. PAPANASTASSIOU, D. A., AND G. J. WASSERBURG, The Rb-Sr Age of a Crystalline Rock From Apollo 16. *Earth Planet. Sci. Letters*, Vol. 16, 1972, pp. 289–298.
102. MURTHY, V. R., M. M. EVENSEN, B. JAHN, AND M. R. COSCIO, JR., Apollo 14 and 15 Samples: Rb-Sr Ages, Trace Elements and Lunar Evolution. *Proc. Third Lunar Science Conference*, Vol. 2, D. Heymann, ed., 1972, pp. 1503–1514.
103. TURNER, G., J. G. HUNEKE, F. A. PODOSEK, AND G. J. WASSERBURG, Ar^{40}-Ar^{39} Systematics in Rocks and Separated Minerals from Apollo 14. *Proc. Third Lunar Science Conference*, Vol. 2, D. Heymann, ed., 1972, pp. 1589–1612.
104. HUSAIN, L., O. A. SCHAEFFER, J. FUNKHOUSER, AND J. SUTTER, The Ages of Lunar Material From Fra Mauro, Hadley Rille, and Spur Crater. *Proc. Third Lunar Science Conference*, Vol. 2, D. Heymann, ed., 1972, pp. 1557–1567.
105. COLEMAN, P. J., JR., B. R. LICHTENSTEIN, C. T. RUSSELL, L. R. SHARP, AND G. SCHUBERT, Magnetic Fields Near the Moon. *Proc. Third Lunar Science Conference*, Vol. 3, D. R. Criswell, ed., 1972, pp. 2271–2286.
106. FULLER, M., Lunar Magnetism. *Rev. Geophys. and Space Phys.*, Vol. 21, 1974, p. 23.
107. NAGATA, T., R. M. FISHER, F. C. SCHWERER, M. D. FULLER, AND J. R. DUNN, Rock Magnetism of Apollo 14 and 15 Materials. *Proc. Third Lunar Science Conference*, Vol. 3, D. R. Criswell, ed., 1972, pp. 2423–2447.
108. PEARCE, G. W., D. W. STRANGWAY, AND W. A. GOSE, Remanent Magnetization of the Lunar Surface. *Proc. Third Lunar Science Conference*, Vol. 3, D. R. Criswell, ed., 1972, pp. 2449–2464.
109. COLLINSON, D. W., S. K. RUNCORN, A. STEPHENSON, AND A. J. MANSON, Magnetic Properties of Apollo 14 Rocks and Fines. *Proc. Third Lunar Science Conference*, Vol. 3, D. R. Criswell, ed., 1972, pp. 2343–2361.
110. GOSE, W. A., A Determination of the Intensity of the Ancient Lunar Magnetic Field. *The Moon*, Vol. 7, 1973, pp. 196–201.
111. RUNCORN, S. K., AND H. C. UREY, A New Theory of Lunar Magnetism. *Science*, Vol. 180, 1973, pp. 636–638.
112. RUNCORN, S. K., D. W. COLLINSON, W. O'REILLY, A. STEPHENSON, M. H. BATTEY, A. J. MANSON, AND P. W. READMAN, Magnetic Properties of Apollo 12 Lunar Samples. *Proc. Roy. Soc. London*, Ser. A., Vol. 325, 1971, pp. 157–174.
113. STRANGWAY, D. W., H. N. SHARPE, W. A. GOSE, AND G. W. PEARCE, Magnetism and the Early History of the Moon. *Lunar Science*, Vol. IV, J. W. Chamberlain and C. Watkins, eds., Lunar Science Institute, Houston, 1973, pp. 697–699.
114. RINGWOOD, A. E., AND E. ESSENE, Petrogenesis of Lunar Basalts and the Internal Constitution of the Moon. *Science*, Vol. 167, 1970, pp. 607–610.

115. GAST, P. W., The Chemical Composition and Structure of the Moon. *The Moon*, Vol. 5, 1972, pp. 121–148.
116. GREEN, D. H., A. E. RINGWOOD, N. G. WARE, AND W. O. HIBBERSON, Experimental Petrology and Petrogenesis of Apollo 14 Basalts. *Proc. Third Lunar Science Conference*, Vol. 1, E. A. King, ed., 1972, pp. 197–206.
117. LORELL, J., G. H. BORN, E. J. CHRISTENSEN, J. F. JORDAN, P. A. LAING, W. L. MARTIN, W. L. SJOGREN, I. I. SHARPIO, R. D. REASONBERG, AND G. L. SCLATER, Mariner 9 Celestial Mechanics Experiment: Gravity Field and Pole Direction of Mars. *Science*, Vol. 175, 1972, p. 317.
118. DOLGINOV, S. S., Y. G. YEROSHENKO, AND L. N. ZHUZGOV, *The Magnetic Field in the Very Close Neighborhood of Mars According to Data From the Mars 2 and Mars 3 Spacecraft*. Goddard Space Flight Center, Report X–690–72–434, 1972.
119. CARR, M. H., Volcanism on Mars. *J. Geophys. Res.*, Vol. 78, 1973, p. 4049.
120. ANDERSON, D. L., Internal Constitution of Mars. *J. Geophys. Res.*, Vol. 77, 1972, p. 789.
121. LEWIS, J. S., Consequences of the Presence of Sulfur in the Core of the Earth. *Earth Planet. Sci. Letters*, Vol. 11, 1971, p. 130.
122. GOETTEL, K. A., Partitioning of Potassium Between Silicates and Sulphide Melts: Experiments Relevant to the Earth's Core. *Phys. Earth Planet. Interiors*, Vol. 6, 1972, p. 161.
123. BRETT, R., and P. M. BELL, Melting Relations in the Fe-Rich Portion of the System Fe-FeS at 30 kb Pressure. *Earth Planet. Sci. Letters*, Vol. 6, 1969, pp. 479–482.
124. MCCAULEY, J. F., M. H. CARR, J. A. CUTTS, W. K. HARTMANN, H. MASURSKY, D. J. MILTON, R. P. SHARP, AND D. E. WILHELMS, Preliminary Mariner 9 Report on the Geology of Mars. *Icarus*, Vol. 17, 1972, pp. 289–327.
125. CARR, M. H., H. MASURSKEY, AND R. S. SAUNDERS, A Generalized Geologic Map of Mars. *J. Geophys. Res.*, Vol. 78, 1973, p. 4031.
126. MASURSKEY, H., An Overview of Geological Results From Mariner 9. *J. Geophys. Res.*, Vol. 78, 1973, pp. 4009–4030.
127. GROSSMAN, L., Fractionation of Refractory Elements in the Solar Nebula (abs.). *Meteoritics*, Vol. 8, 1973, p. 41.
128. GREEN, D. H., and A. E. RINGWOOD, Mineralogy of Peridotitic Compositions Under Mantle Conditions. *Phys. Earth Planet. Interiors*, Vol. 3, 1969, p. 359.
129. USSELMAN, T. M., Composition and Temperature of an Fe-Ni-S Core of the Earth (abs.). *EOS, Trans. Am. Geophys. Union*, Vol. 55, 1974, p. 337.
130. CAMPBELL, D. B., R. B. DYCE, R. P. INGALLS, G. H. PETTENGILL, AND I. I. SHAPIRO, Venus: Topography Revealed by Radar Data. *Science*, Vol. 175, 1972, p. 514.
131. DAVIDSON, G. T., AND A. D. ANDERSON, Venus: Volcanic Eruptions May Cause Atmospheric Obscuration. *Science*, Vol. 156, 1967, p. 1729.
132. WEERTMAN, J., Venus: Tectonic Activity. *Science*, Vol. 156, 1967, p. 395.
133. HIGGINS, G., AND G. C. KENNEDY, The Adiabatic Gradient and the Melting Point Gradient in the Core of the Earth. *J. Geophys. Res.*, Vol. 76, 1971, p. 1870.
134. BIRCH, F., Energetics of Core Formation. *J. Geophys. Res.*, Vol. 70, 1965, p. 6217.
135. FLASAR, F. M., AND F. BIRCH, Energetics of Core Formation: A Correction. *J. Geophys. Res.*, Vol. 78, 1973, p. 6101.
136. TRASK, N. J., Preliminary Results of Television Reconnaissance of Mercury (abs.). *EOS, Trans. Am. Geophys. Union*, Vol. 55, 1974, p. 340.
137. BEHANNON, K. W., R. P. LEPPING, N. F. NESS, K. H. SCHATTEN, AND Y. C. WHANG, Magnetic Field Observations With Mariner 10 (abs.). *EOS, Trans. Am. Geophys. Union*, Vol. 55, 1974, p. 340.